Chem Soc Rev

Metallosupramolecular receptors for fullerene binding and release

Journal:	*Chemical Society Reviews*
Manuscript ID	CS-SYN-04-2015-000315.R2
Article Type:	Tutorial Review
Date Submitted by the Author:	28-Sep-2015
Complete List of Authors:	García-Simón, Cristina; Universitat de Girona, Institut de Química Computacional i Catàlisi (IQCC) and Departament de Química Costas, Miquel; Universitat de Girona, Institut de Química Computacional i Catàlisi (IQCC) and Departament de Química Ribas, Xavi; Universitat de Girona, Institut de Química Computacional i Catàlisi (IQCC) and Departament de Química

Metallosupramolecular receptors for fullerene binding and release

Cristina García-Simón, Miquel Costas* and Xavi Ribas*

Key Learning Points box.

a) Supramolecular hosts for fullerene encapsulation
b) Strategies for enhancing fullerene binding in supramolecular hosts
c) Strategies for fullerene release from supramolecular hosts
d) Fullerene purification strategies using supramolecular hosts

1. Introduction

1.1. Relevance of fullerene separation.

Fullerenes are the third most stable allotrope of carbon and in contrast to graphite or diamond, that are infinite extended arrays of sp^2- and sp^3-hybridized carbon atoms, respectively, fullerenes are spherical discrete molecules which contain a defined number of Csp^2 atoms. Consequently fullerenes are soluble in various organic solvents, an essential requirement for chemical manipulations. These spherical molecules were first observed experimentally by Kroto and Smalley in 1985.[1] The finding of fullerenes opened a gateway towards the discovery of other carbon nanoforms such as carbon nanotubes, graphene, nano onions, peapods, *etc*.

Fullerenes and their derivatives present a wide range of applications highlighting their use in materials science (polymers, thin films, liquid crystals, *etc*),[2] electroactive materials in solar cells,[3] superconductivity[4] and biological applications[5]. However, all these applications are limited in origin by the current tedious and expensive methodologies for selective purification of fullerenes.

The crude product generated usually by arc discharge or laser vaporization on carbon sources contains mixtures of fullerenes of different sizes, as well as other carbon allotropes such as carbon nanotubes and amorphous forms of carbon. The first examples reported for the purification of fullerenes were based on controlled sublimation of the carbon soot.[6] Other common methods to separate fullerenes from soot consist in extraction with organic solvents or the purification by crystallization. Currently, chromatographic techniques are predominantly used for the purification of fullerenes. Alumina, graphite, activated carbon, polystyrene gel or γ-cyclodextrines have been used as stationary phases.[7] In spite of the fact that efficient columns for the HPLC separation of fullerenes are available (COSMOSIL© columns), most of the methods mentioned here require enormous amounts of solvent and can cause fullerene decomposition, irreversible absorption of fullerenes within the stationary phase, or give moderate yields. Furthermore, these methods are often tedious, energy and time-consuming, and in some cases, it is difficult to obtain specific fullerenes with high selectivity in a pure form. Therefore, designing an improved fullerene purification methodology is a challenging and desired goal.

1.2. Molecular hosts to selectively entrap fullerenes

The use of molecular receptors for fullerene separation in solution has emerged as an attractive alternative since it allows potential selectivity, no specific equipment is required and ideally, recyclable hosts can be designed. Additionally, the encapsulation promotes the solubilisation and chemical modification of fullerenes. It also facilitates the selective extraction of higher fullerenes and their chiral resolution.[8]

In this tutorial review some examples of relevant fullerenes receptors will be described. The attention has been focused towards supramolecular receptors based on coordination bonds. Nevertheless, some examples of covalent and other supramolecular receptors will also be discussed in the following sections.

1.2.1 Enhanced fullerene binding

The fullerene structure is based on an extended π-system, containing carbon atoms with a sp^2 hybridization, and their reactivity is typical of an electron deficient olefin.

In order to design a molecular receptor for the selective separation of fullerenes, the most important factor to take into account is the complementarity between the host and

the fullerene. On one hand structural complementarity needs to be considered (*i.e.* size and shape of the receptor), and on the other hand the electronic complementarity also plays a crucial role. For this reason, the majority of molecular hosts for fullerenes described so far are based on extended π-systems (i.e. π-extended tetrathiafulvalenes or porphyrins) which tend to act as π-donor moieties, favouring the interaction with fullerenes that behave as π-acceptor moieties.[9] Another important factor to consider when designing a fullerene receptor is the structural and electronic tunability of the container. A tuneable and versatile receptor may pave the way for reaching a good selectivity towards a specific fullerene within a mixture of fullerenes of different sizes. A host molecule can also be tuned in order to selectively encapsulate a particular higher fullerene or an endohedral fullerene. Besides other factors such as solvophobic effects may also condition the fullerene-receptor interaction, and they also need to be considered.

1.2.2 Covalent receptors for fullerene recognition

Traditional covalent chemistry has led to the synthesis of sophisticated molecular receptors for fullerenes recognition. Remarkably, highly stable host-guest adducts, with association constants $>10^9$ M^{-1}, have been obtained using covalent host platforms.

1.2.2.1 Fully organic covalent hosts

Ringsdorf and Wennerström reported the first examples of covalent molecular receptors for fullerenes in 1992. They complexed fullerenes using aza-crown compounds and γ-cyclodextrins.[10,11] Since then, a number of covalent fully organic receptors have been reported in the literature. For example, arene based receptors such as cyclodextrins (CD),[12] calixarenes[13] and cyclotriveratrylenes (CTV's)[14] have proven to be efficient receptors for fullerenes, especially when two or more of these units are associated, through the formation of cage-like receptors (*vide infra*). There are also arene-based fullerene receptors such as cycloparaphenylenes or carbon nanotubes (CNTs), which can give rise to peapod structures.[15] Another relevant example was reported by Martín who used π-extended derivatives of tetrathiafulvalene (exTTF) to wrap around different fullerenes.[8] Multiple examples of fully organic fullerene receptors have been reported so far and as such an extensive account is beyond the purpose of this review paper. Herein we will focus mainly on fully organic receptors having a 3D cage-

like structure.

The suitability of dimeric cyclotriveratrylene (CTV)-based cage-like structures for fullerene separation was exemplified by Chiu and co-workers who synthesized a cage formed by two covalently linked CTV units (**1**) (Figure 1a). Zig-zagging alkyl chains were chosen as spacers in order to minimize the energy cost of structural reorganization during the guest binding event. Notably, receptor **1** is able to encapsulate C_{60} and C_{70} fullerenes at room temperature.[16] The cage favours the formation of the hemicarceplex containing C_{70} in presence of C_{60} and therefore, the system could be applied in the selective encapsulation of C_{70} from fullerene extracts. To a solution of **1** in tetrachloroethane (TCE), fullerene extract was added and the mixture was heated to 313 K for 16h, thereafter host-guest adducts with the C_{70} fullerene were exclusively formed.

Very recently it was demonstrated that covalent cage **1** encapsulates $Sc_3N@C_{80}$ metallofullerene under solvent-free conditions. $Sc_3N@C_{80}$ exhibits two structural isomers D_{5h} and I_h.[17] The lack of solubility of these higher fullerenes makes their isolation and characterization challenging tasks. Moreover, the lack of hydrogen atoms present in their structure prevents their study by ^{1}H-NMR. Consequently, ^{13}C-NMR, a less sensitive technique, is the most widely used technique for directly identifying the fullerene isomers. When $Sc_3N@C_{80}$ was sequestered inside cage **1**, the ^{1}H-NMR displayed two set of signals that were attributed to **[**$Sc_3N@D_{5h}$-C_{80}]⊂**1** and [$Sc_3N@I_h$-C_{80}]⊂**1** adducts. Despite of the fact that the solubility of the endofullerene in TCE was increased by approximately 50 times upon encapsulation, it was still too poor to permit its further characterization by ^{13}C-NMR. The authors therefore decided to synthesise the more soluble cage **2** which contained three succinic diester linkages (Figure 1b). The enlarged cage **2** was able to encapsulate $Sc_3N@C_{80}$ and a crystal structure was obtained for the [$Sc_3N@C_{80}$]⊂**2** adduct (Figure 1c), which confirmed the Russian doll (Matryoshka)-like multilayer structure. Remarkably, when $Sc_3N@C_{80}$ was encapsulated within cage **2**, its solubility in TCE was 200 times greater than that of the free endofullerene, allowing its characterization by ^{1}H-NMR and ^{13}C-NMR. The ^{13}C-NMR spectrum corresponding to [$Sc_3N@C_{80}$]⊂**2** allowed for identification of the hemicarceplexes of both $Sc_3N@D_{5h}$-C_{80} and $Sc_3N@I_h$-C_{80} isomers, which appear in a 1:4 ratio respectively. Moreover, the ^{1}H-NMR spectrum also displayed two set of signals of the aromatic C-H proton nuclei of the CTV units in the same 1:4 ratio.

-insert Figure 1 here-

Figure 1. Chemical structure of the CTV-based molecular cage **1** and **2** (**a** and **b**).[16] **c**) Representation of the solid state structure of the $[Sc_3N@C_{80}]\subset$**2** host-guest adduct (hydrogen atoms are omitted for clarity).[17]

Most of the fully organic covalent hosts for fullerenes reported on the literature are constructed via irreversible chemical reactions, which generally involve tedious and often low yielding complex synthetic procedures. Interestingly, recent advances in dynamic covalent chemistry (DCC), which takes advantage of reversible reactions such as alkyne methatesis/condensation, offers appropriate pathways to high-yielding synthesis of covalent organic capsule-like receptors. Strikingly in 2011, Zhang developed a shape persistent capsule containing non-metalated porphyrin units making use of DCC.[18] The rectangular prismatic cage (**4**) was synthesised *via* alkyne metathesis of two tetrasubstituted porphyrins (**3**). Interestingly, the cage forms 1:1 complexes with C_{60} and C_{70} fullerenes, when the cage is mixed with fullerenes in toluene at room temperature (Figure 2). It is well known that there is a favoured donor-acceptor interaction between porphyrins and fullerenes (*vide infra*). The rigidity of host **4** along with its combination of conjugated systems results in a cage with a 3 orders of magnitude higher affinity towards C_{70} ($K_a = 1.5 \cdot 10^8\ M^{-1}$) compared to C_{60} ($K_a = 1.4 \cdot 10^5\ M^{-1}$). The significant difference in affinity of the cage towards C_{70} over C_{60} facilitated the selective separation of C_{70} fullerene from a mixture containing both fullerenes.

-insert Figure 2 here-

Figure 2. Top: tetrasubstituted porphyrin (**3**), used for the preparation of covalent capsule **4** reported by Zhang. Bottom: schematic representation of the construction of capsule **4** by alkyne metathesis, and subsequent encapsulation of the fullerene.[18]

1.2.2.2. Metal containing covalent hosts

Metalloporphyrins contain a large π-conjugated system, thus they tend to act as π-donor moieties. Conversely, fullerenes behave as π-acceptors and this electronic complementarity favours the interaction between these two molecules.[19] Nevertheless, this interaction is weak in solution and is difficult to visualize spectroscopically. For this reason, several examples of fullerene hosts containing two or more metalloporphyrin units have been reported in the literature, making attempts to enhance the strength of this fullerene-host interaction.[8,20–23]

One of the most well-known examples of fullerene receptors bearing

metalloporphyrins, was reported by Aida in 1999. The authors reported the synthesis of a covalently linked cyclic dimer of zinc(II) porphyrins (**5**) (Figure 3).[24] This cyclic host formed a highly stable 1:1 inclusion complex with C_{60} in benzene at room temperature ($K_a = 6.7 \cdot 10^5$ M^{-1}). Remarkably, in analogous experiments using C_{70} fullerene, an association constant 30 times larger than that of C_{60} ($K_a(C_{70}) \sim 10^7$ M^{-1}) was obtained. It appears that C_{70} adopts a side-on conformation with respect to the two metalloporphyrin moieties in order to maximize the π-stacking interactions. With the intention to obtain more stable host-guest adducts, the authors modified the receptor structure by changing: i) the porphyrin substituents, R, which could modify the π-basicity of the porphyrin or its conformation; ii) the linker parts (Z) in order to gain flexibility or rigidity (aliphatic or acetylenic chains); iii) the metal ions of the porphyrin moieties. It was observed that hydrogenated separators (Z) gave more flexible structures (**5_a** more flexible than **5_c**), and facilitated the host-guest interaction. Furthermore, when the porphyrin contains a more concave conformation (i.e. β-pyrrole-substituted porphyrin, host **5_b**) the host-guest contact is improved. Finally it was observed that the metal ions which gave highest association constants are those belonging to group 9 of the periodic table. Strikingly, the rhodium(III) porphyrin dimer showed an affinity 100 times higher towards C_{60} and C_{70} than its zinc(II) analogue.[25] Furthermore, in the case of the iridium(II) porphyrin cyclic dimer the association constant for C_{60} and C_{70} in benzene, was too large to be evaluated accurately ($K_a > 10^9$ M^{-1}). Studies in the solid state (XRD) and in solution (NMR), at low temperature, indicated that dynamic organometallic bonds between the iridium(II) metal ions from the porphyrins and the π-electron-rich 6:6 junctions from the fullerenes were formed. This metal-fullerene interaction caused an ellipsoidal deformation of the C_{60} and an end-on orientation of C_{70} relative to the porphyrin units.[26] Finally, the authors successfully used the different binding ability of the hosts towards the fullerenes to perform the selective extraction of higher fullerenes ($\geq C_{76}$) from fullerene mixtures.[27]

-insert Figure 3 here-

Figure 3. Top: molecular structure and formulae of metalloporphyrin dimer **5** reported by Aida.[20]

The same authors later reported in 2011 the synthesis of a new cyclic receptor based on copper(II) or zinc(II) metalloporphyrins (**6_{cyclo}**), which could be transformed into the cubic-cage (**6_{cage}**) analogue by intramolecular ring-closing olefin metathesis (Figure

4).[28] Both structures were able to encapsulate La@C_{82} endofullerene in toluene at 25ºC (K_a ~10^6-10^7 M^{-1}). The inclusion experiments using the cyclic receptors based on copper(II) paramagnetic porphyrins, showed ferromagnetic coupling with the paramagnetic La@C_{82} fullerene. However, a ferrimagnetic coupling was observed when the receptor was transformed into its cage analogue. This change in spin coupling was rationalized by the change in the geometry of the host-guest complex.

-insert Figure 4 here-

Figure 4. Representation of the molecular structure of [La@C_{82}]⊂**6**$_{cyclo}$ and [La@C_{82}]⊂**6**$_{cage}$, and their transformation by ring-close metathesis. Adapted with permission from (Ref. [28]). Copyright (2011) American Chemical Society.

A different example of cyclic porphyrin dimers was investigated by Ballester. Cyclic covalent receptors were synthesized by dimerization of two non-*β*-pyrrole-substituted mono porphyrins, bearing four meso-aryl substituents (**7**), to give **8** (Figure 5).[21] Subsequently, hydrogenation of **8** afforded the flexible cyclic dimer **9**. As Aida had observed previously in their receptors, the relative rigidity of the spacer units affected the shape and flexibility of the hosts and controlled their affinity towards different fullerene guests. Both receptors **8** and **9** form 1:1 host-guest adducts with C_{60} and C_{70} fullerenes at room temperature using toluene (TL) or dichloromethane (DCM) as solvents. The more rigid receptor **8**, which bears fully unsaturated spacers (six carbon acetylenic chains), presented a relatively weak interaction with C_{70} ($K_{a(DCM)}$ ~10^4 M^{-1} and $K_{a(TL)}$ ~10^4 M^{-1}) and an unobservable interaction with C_{60} (K_a < 10^3 M^{-1}). On the other hand, the more flexible host **9**, containing fully saturated six-carbon linkers, forms more stable complexes with C_{60} ($K_{a(DCM)}$ ~10^4 M^{-1} and $K_{a(TL)}$ ~10^4 M^{-1}) and C_{70} ($K_{a(DCM)}$ ~10^5 M^{-1} and $K_{a(TL)}$ ~10^4 M^{-1}) due to better adaptability. The host-guest adducts with both **8** and **9** receptors, were also characterized in the solid state. In collaboration with Echegoyen the authors discovered that both dimers were also able to form inclusion complexes with Sc_3N@C_{80} endofullerene (K_a ~10^5). For the first time, solid state structures were obtained for an endohedral fullerene bound to molecular *bis*-porphyrin receptors.[29]

-insert Figure 5 here-

Figure 5. Molecular structure of the substituted zinc(II) porphyrin **7** used by Ballester to prepare covalent dimers **8** and **9**. Reproduced in part from {Ref. 21} with permission of John Willey and Sons.

The association constant between fullerenes and porphyrins dramatically increased when using porphyrin dimers (*vide supra*) instead of a single porphyrin. In response, different research groups worked on the development of multiple-porphyrin systems with the aim of achieving even higher association constants.[22] An interesting example was reported by Anderson who developed a cyclic porphyrin trimer that presented a high affinity for fullerenes (Figure 6a). The rigid cyclic porphyrin trimer (**10**) was synthesized by Sonogashira coupling of 3,4-diiodophthalimide and the alkyne-terminated linear porphyrin trimer. The linear porphyrin trimer was synthesized following an elaborated synthetic protocol.[22] The trimeric receptor **10**, formed 1:1 host-guest adducts with C_{60} at room temperature in different organic solvents (*i.e.* toluene). The association constant for $C_{60}\subset$**10** in toluene was $(1.6\pm0.7)\cdot10^6$ M^{-1}. On the other hand, the inclusion compound with C_{70} was two orders of magnitude more stable than with C_{60} (K_a (C_{70})= $(1.6\pm0.7)\cdot10^8$ M^{-1}. The receptor also formed 1:1 adducts with higher fullerene C_{86} and La@C_{82} endofullerene, however, adducts are too stable for the equilibrium constant to be calculated by UV-Vis or fluorescence titrations (K_a >10^9 M^{-1}). The value obtained for the association constant between the cyclic trimer and C_{60} in toluene is slightly higher than the ones obtained for zinc(II)-porphyrin dimers, indicating that the presence of the third porphyrin moiety has a positive effect on the affinity towards C_{60}. The effect of the third porphyrin is more relevant for C_{70} and higher fullerenes. The association constant of $C_{70}\subset$**10** is much higher than those reported for other zinc(II) porphyrin hosts and the association constant for $C_{86}\subset$**10** and La@$C_{82}\subset$**10** is still higher, therefore the larger size of the fullerene enables them to better interact with the three walls of the receptor.

With these results in hand Osuka, Shionokubo and Aratani further increased the number of porphyrin units in order to improve the fullerene-porphyrin interaction. The authors synthesized the nanobarrel **11** bearing four porphyrin units (Figure 6b), following a concise synthetic route. The addition of C_{60} to a solution of **11** in toluene, at room temperature, gave 1:1 inclusion adducts.[23] Unexpectedly, the association constant for $C_{60}\subset$**11** calculated from UV-vis titrations in toluene was $(5.3\pm0.1)\cdot10^5$ M^{-1}, which is slightly smaller than those reported for cyclic porphyrin dimers and Anderson's trimer. The lower value for the association constant was rationalized by the high rigidity of this covalent receptor, which in this case is detrimental. Nevertheless, the host-guest adduct structure was unambiguously confirmed by X-Ray diffraction studies (Figure 6c).

-insert Figure 6 here-

Figure 6. a) Molecular structure of the cyclic porphyrin trimer **10** synthesized by Anderson. Adapted with permission from (Ref. 22). Copyright (2012) American Chemical Society. **b)** Structure of nanobarrel **11**. Adapted with permission from (Ref. 23). Copyright (2010) American Chemical Society. **c)** Lateral and top view of the X-ray crystal structure of C_{60}⊂**11** (hydrogen atoms have been omitted for clarity).

1.2.3 Supramolecular receptors for fullerene binding

As the scale and sophistication of the fullerene receptors increased, the synthetic protocols based on traditional covalent chemistry required large synthetic and purification efforts, and typically resulted in low yields. Supramolecular chemistry allows for the construction of highly complex functional systems in a straightforward manner and good yields. For these reasons the use of supramolecular approaches in the preparation of host platforms for fullerene recognition has undergone extraordinary development during the past years.

Weak non-covalent interactions such as hydrogen bonds, van der Waals forces or π-π interactions have been used to hold the molecular building blocks together in order to form sophisticated supramolecular receptors. Moreover, some interactions that possess a significant covalent bond component (e.g. coordination metal-ligand bonds) are also widely used. In this review article special attention will be given to fullerene receptors based on metal-ligand coordination bonds.

1.2.3.1. Hydrogen bonded hosts

The suitability of dimeric CTV cage-like structures for fullerene separation was also exemplified by Mendoza who prepared a nanocapsule (**13**) by self-assembly, utilizing hydrogen bonding between two CTV (**12**) units that were modified with three high-affinity hydrogen-bonding units (1,1'-carbonyldiimidazole) (Figure 7). This nanocapsule presents affinity towards C_{60} (K_a (C_{60})= $1.82 \cdot 10^3$ M^{-1}) and C_{70} (K_a (C_{70})= $3.89 \cdot 10^4$ M^{-1}).[30] The higher affinity towards C_{70} was rationalized through an improved hydrogen-bonding interaction among the CTV units, giving rise to a more stable host-guest adduct. In contrast to the covalent CTV-based cage reported by Chiu and co-workers, which presents a more rigid structure, nanocapsule **13** presents a very flexible structure that allows for the encapsulation of higher fullerenes up to C_{84}. When the capsule is reacted with fullerene extract (~ 2% higher fullerenes), host-guest adducts with C_n (60, 70, 76, 78, 82 and 84) were observed by HPLC.[31] Taking advantage of the different binding affinities and by changing the rations of nanocapsule/fullerene extract,

the authors were able of selectively extracting C_{70} and C_{84} fullerenes.

-insert Figure 7 here-

Figure 7. Top: CTV unit (**12**) used for the preparation of the supramolecular capsule **13** reported by Mendoza. Bottom: reaction scheme for the encapsulation and liberation of fullerenes using **13**.[30]

1.2.3.2 Fullerene hosts assembled through coordination bonds.

When the complexity of the target supramolecular receptors increases, the assembly of small molecules into larger aggregates may turn into an increasingly impeded process. This is mostly a result of the lack of control during the self-assembly process. As a response to these limitations, coordination-driven self-assembly has emerged as a powerful tool to regain control over supramolecular synthesis. It facilitates the formation of large complex molecules, ranging from ~300 $Å^3$ to more than 2000 $Å^3$.[32]

The strength of coordination bonds is between that of a weak traditional supramolecular interaction and that of a strong covalent bond. Metal-ligand interactions offer a high degree of directionality as a result of predictable metal-ion coordination geometries. In addition, the diversity of transition metal complexes and ligands available as building blocks makes this strategy very versatile, allowing the generation of multiple supramolecular structures.

Over the years different supramolecular synthetic approaches have been developed based on coordination bonds. The most widely used strategies are the directional bonding (DBA), molecular panelling (MPA) and symmetry interaction (SIA) approaches. In addition, weak link (WLA) and bimetallic building block (DBBA) approaches have also lead to complex coordination supramolecules. The corresponding literature has been extensively gathered in excellent reviews (see refs: 32) and will not be exhaustively discussed in this article.

The predictable directionality and geometry of metal-ligand coordination bonds have been used to synthesize the vast majority of the reported coordination supramolecular structures for fullerene recognition (2D and 3D), which usually are highly symmetric and resemble Archimedean or Platonic solids in shape. However, there are also structures with lower symmetry that have also been used as host for fullerene separations (i.e. heteroleptic species) and will also be described hereafter.[33]

Finally, apart from the metal-ligand interaction itself, there are other factors to

consider which play a crucial role in the development of coordination receptors, such as the counter anions in charged species, labilization agents, guest templates or solvent interactions. In many cases these subtle secondary interactions play a key role in the encapsulation of the fullerene.

2. 2D coordination receptors for fullerene recognition.

The examples of coordination supramolecular polygons capable of interacting with fullerenes remain scarce, most likely due to the limited fullerene-receptor surface interaction (K_a up to 10^5 M^{-1}). Nevertheless, some elegant examples of bi-dimensional coordination structures capable of hosting fullerenes have been reported in the literature.[34–36]

2.1 Aromatic heterocycles for fullerenes binding

In 2012 Sallé reported on the synthesis of molecular triangles (**15**) and squares (**16**), obtained from metal-ligand directed self-assembly of *cis*-blocked square planar Pt(II) complexes and BPTTF-based electron-rich ligands (**14**, BPTTF: bis(pyrrolo)tetrathiafulvalene) (Figure 8).[34] When an equimolar mixture of ligand **14** and (*dppp*)Pt(CF_3SO_3)$_2$ were mixed in dichloromethane both species **15** and **16** were generated, in a 2:1 ratio. The two species were easily separated by filtration and solvent evaporation. Whilst the square **16** is too large to accommodate electron-deficient C_{60} (cavity size ~20 Å), UV-vis experiments indicated that triangle **15** encapsulates C_{60} with a ~10^4 M^{-1} association constant. The rigid and pre-organized structure of **15**, with an inner cavity size of ~13 Å, and the cooperative electron-donating ability of the three moderate π-extended BPTTF units, favors the interaction between the receptor and the substrate.

-insert Figure 8 here-

Figure 8. Chemical formula and schematic representation of ligand **14** (top) used for the self-assembly of coordination polygons **15** and **16** (bottom).[34]

In parallel studies Chi, Stang and Mukherjee worked on the synthesis of a 2D-metallamacrocycle that was also able to bind C_{60}. The 2D coordination receptor was obtained from [2+2] self-assembly of carbazole-based 90º dipyridyl donor 3,6-di(4-pyridylethynyl)carbazole ligand (**17**) and *cis*-capped (*dppf*)Pd(CF_3SO_3)$_2$ complex (Figure 9).[35] Host **18** was prepared under mild conditions when an equimolar mixture of ligand **17** and *cis*-(*dppf*)Pd(CF_3SO_3)$_2$ were stirred for 5h in nitromethane at 50ºC. Crystals suitable for single X-Ray diffraction were obtained and the resulting structure showed a bowl-shaped conformation which is optimum for the interaction with the convex surface of the fullerene (Figure 9b). During fluorescence titration of the C_{60}-**18**

adduct, the intensity of the band corresponding to **18** (λ_{max}=372) depleted rapidly upon addiction of C_{60} (Figure 9c). This quenching effect was rationalized by the formation of the $C_{60}\subset$**18** inclusion compound. Analysis of the fluorescence titration data gave a value of the association constant of ~10^5 M^{-1}, which is indicative of the formation of a stable host-guest adduct.

-insert Figure 9 here-

Figure 9. a) Chemical formula of compounds **17** and *cis*-capped Pd(II) complex, *cis*-(*dppf*)Pd(CF_3SO_3)$_2$. **b)** Self-assembled coordination bowl **18. c)** Quenching of the emission intensity of macrocycle **18** upon the gradual emission of C_{60} fullerene. Adapted with permission from (Ref. 35). Copyright (2012) American Chemical Society.

2.2 π-extended systems

Recently, Yoshizawa and co-workers used a pyridine curved ligand **19**, bearing large aromatic panels (two anthracene molecules linked by *m*-phenylene), and silver(I) as metal for the coordination-driven self-assembly of the tube-like receptor **20**.[36] The tubular host **20** was exclusively formed upon reaction of ligand **19** and $AgNO_3$, in presence of C_{60} in acetonitrile during 1 hour at room temperature in the dark, whereby the colour of the solution changed from yellow to red-purple (Figure 10). C_{60} plays the role of a template molecule and as a result 1:1 host-guest adducts were formed. Silver(I) anions adopted a linear geometry forming complexes with two ligands (M_2L_2). Thanks to its open structure receptor **20** was also able to encapsulate different C_{60}-malonate and -indene derivatives, although no K_a was reported.

-insert Figure 10 here-

Figure 10. Chemical formula and schematic representation of ligand **19** (**a**) used for the self-assembly of tubular receptor **20** (**b**).[36]

3. 3D metallocages to entrap fullerenes.

In contrast to bi-dimensional metalloreceptors, three-dimensional hosts offer a more confined environment to accommodate and isolate fullerenes. Besides, more ligand units can be incorporated in the structure further extending the receptor-fullerene surface contact, which translates into much higher association constants (K_a up to 10^8). As previously mentioned, the metal-ligand interaction allows for the construction of fullerenes receptors in a straightforward manner, and it permits the fine tuning of the

receptor geometry or solubility. Additionally, coordination 3D structures present a more flexible and adaptable structure than the covalent ones, facilitating the interaction with the fullerene substrate. For all these reasons, the attention of several research groups has been directed towards the use of the coordination-driven self-assembly approach to build sophisticated 3D cage-like receptors capable of catching fullerenes and herein, some examples will be highlighted.[33,37–48]

3.1 Coordination cage-like receptors containing π-extended moieties

Different π-extended systems such as calixarenes and resorcinarenes have also been used as molecular building blocks in the preparation of coordination cages for the isolation of fullerenes.[37] As for the case of CTV units, these species can also establish a donor-acceptor interaction with fullerenes.

One of the first examples of a coordination 3D cage-like receptor for fullerenes was reported in 1999 by Shinkai.[37] The authors targeted the synthesis of a dimeric calix[n]arene cage for fullerene inclusion, by self-assembly through coordination bonds. Calixar[3]arenes units substituted with 3 pyridine moieties were reacted with $[Pd^{II}(Ph_2PCH_2CH_2PPh_2)](CF_3SO_3)_2$ in a 2:3 ratio, to form the molecular cage **21** (Figure 11a). The nanocapsule forms 1:1 host-guest adducts with C_{60} at 25ºC in 1,2-dichloroethane (K_a ~50 M^{-1}). Afterwards it was discovered that the K_a for C_{60} was remarkably increased when lithium cations were bound to the ester lower rims of capsule **21**, giving a new complex Li-**21**.[49] In the Li-**21** capsule the phenyl groups are more flattened than those in **21**, in such a way that the three ethoxycarbonylmethoxy groups can interact with the bound lithium cation, improving the interaction between the fullerene and the calixarene walls (K_a ~$2 \cdot 10^3$ M^{-1} in 1,2-dichloroethane at 25ºC). Interestingly, when the bigger sodium cation interacts with the esters pockets to give Na-**21**, the phenyl groups stand up, which tapers the cage structure and as a consequence the cage adopted an ellipsoidal shape which impeded the inclusion of the C_{60} fullerene (K_a ~5 M^{-1} in 1,2-dichloroethane at 25ºC) (Figure 11b). This modification of the cage shape and size induced by cation binding was revealed as a good strategy for the controlled binding and release of the encapsulated C_{60}.

-insert Figure 11 here-

Figure 11. a) Chemical structure and schematic representation of the coordination cage **21** reported by Shinaki and co-workers. **b)** Flattening of the homocalix[3]arene units induced by lithium cations, and release of C_{60} induced by the interaction with sodium cations. Adapted with permission from (Ref. 37). Copyright (1999) American Chemical Society.

Taking advantage of the predictability and high directionality of the pyridine-N···Pd coordination bond, and using subphthalocyanine substituted with pyridines (**22**) as building blocks, Torres reported on the synthesis of a library of M_3L_2 metallic cages suitable for the encapsulation of fullerenes (Figure 12). Subphthalocyanines (SubPcs) have a concave geometry comprising of a 14 π-electron core able to interact with fullerenes.[50] The synthesis of metallocages with a C_3 symmetry (**23$_{a-e}$**) was performed by mixing stoichiometric amounts of SubPc (**22**) and the corresponding palladium(II) or platinum(II) complex and stirring the solution in DCM under reflux. First a cage containing ethylenediamine as a ligand and palladium(II) as the metal was reported (**23$_a$**). In solution the cage revealed the presence of two diastereoisomers which slowly exchange until reaching a thermodynamic equilibrium. Cages **23$_{b-e}$** were prepared by self-assembly of palladium(II) or platinum(II) metal ions and phosphine ligands, which in turn allowed their characterization by ^{31}P NMR. The host-guest adduct between capsule **23$_a$** and C_{60} was formed by adding 5 equivalents of the fullerene to a previously equilibrated solution of the host in acetone at room temperature. The formation of 1:1 (**23$_a$**⊂C_{60}) complex was confirmed by NMR and ESI-MS experiments. The encapsulation in acetone dramatically increases the solubility of the fullerene in this solvent, which makes the capsule of potential interest as a phase-transfer catalyst for C_{60}. Host-guest experiments with cages **23$_{b-e}$** under the same conditions (acetone, r.t.) also gave 1:1 host guest adducts with C_{60}, C_{70}, [6,6]-phenyl-C_{61}-butyric acid methyl ester ([60]PCBM) and [6,6]-phenyl-C_{71}-butyric acid methyl ester ([70]PCBM) fullerenes. These experiments were also performed following a fullerene template approach.[38] Initially, SubPc (**22**) was stirred with the fullerene for one hour and subsequently the metal complex was added. The association constants for [60]PCBM and [70]PCBM were calculated by monitoring changes in the NMR spectra. Unfortunately, for the palladium(II) cages the equilibrium was too fast and no significant shifts were observed upon addition of the fullerenes. For the platinum(II) analogues (**23$_{d-e}$**), the K_a for **23$_d$** was found to be $4.6 \cdot 10^4$ M^{-1} and $1.5 \cdot 10^5$ M^{-1} for [60]PCBM and [70]PCBM, respectively, and $3.2 \cdot 10^2$ M^{-1} and $2.2 \cdot 10^3$ M^{-1} for [60]PCBM and [70]PCBM for **23$_e$**. [70]PCBM forms more stable adducts with the capsules because its size is more appropriate for interaction with the cage.

-insert Figure 12 here-

Figure 12. Representation of the self-assembly reaction between SubPc (**22**) and the corresponding metal complexes, to give the coordination cage **23**. Cages $\mathbf{23_{a\text{-}e}}$ encapsulate different fullerenes in acetone (en = ethylenediamine, dppp = 1,1'-bis(diphenylphosphino)propane and dppf = 1,1'-bis(biphenylphosphino)ferrocene).[38]

Yoshizawa and co-workers, moved from 2D receptors (Figure 10) to 3D receptors by changing the metal ions used for the self-assembly reaction (Figure 13). Unlike silver (I) ions, palladium (II) adopted a distorted square planar geometry with four ligands (M_2L_4). The coordination 3D cage **24** was obtained by self-assembly of ligand **19** (see Figure 10) and $Pd(NO_3)_2$ in DMSO at 100ºC.[39] The large aromatic panels (two anthracene molecules linked by *m*-phenylene) of ligand **19** provided an aromatic shell that possess an enclosed cavity which can facilitate stronger host-guest interactions in comparison with receptor **20** (Figures 10 and 13a). Interestingly the cage cavity was large enough (~1 nm in diameter) for the encapsulation of large guest molecules. The reaction between cage **24** and an excess of C_{60} in acetonitrile at 80ºC for 3 h, gave 1:1 host-guests complexes. The palladium(II) based cage irreversibly binds C_{60} through π-stacking interactions (Figure 13b). Remarkably, cage **24** showed selective molecular recognition abilities and could only encapsulate C_{60} of complementary shape and size, from a mixture of C_{60} and C_{70}.

Afterwards, the same authors reported on the synthesis of a new cage **25** analogous to **24** in which mercury(II) metal ions were used as nexus.[40] This M_2L_4 capsule easily interconverts to a tube-like structure **26** (analogous to **20**) in response to modulation of the metal-to-ligand ratio (Figure 10 and 13c). When ligand **19** and $Hg(CF_3SO_3)_2$ were mixed in a 2:1 ratio in acetonitrile at room temperature for 5 min, nanocapsule **25** was obtained. On the other hand, if the curved ligand **19** and $Hg(CF_3SO_3)_2$ were mixed in a 1:1 molar ratio under similar conditions, 2D receptor **26** was obtained. Both structures were fully characterized by means of NMR, ESI-MS and XRD. Fast interconversion between the cage-like structure **25** and the tube **26** was achieved by changing the metal-to-ligand ratio, by the addition of further equivalents of the ligand or the metal ion. When 2 equivalents of the mercury(II) salt were added to 1 equivalent of cage **25** (M_2L_4), the cage changed its conformation to give two units of tube **26** (M_2L_2), in 15 min at room temperature in acetonitrile. Additionally, tube **26** was quickly transformed to cage **25** by adding 2 equivalents of ligand **19** for each equivalent of tube. In spite of the fact that both receptors **25** and **26** possess large inner cavities with similar diameters (~1 nm) they present different affinities towards fullerenes. When a colourless solution

of capsule **25** in acetonitrile was mixed in a 1:3 ratio with fullerene C_{60} at room temperature for 15 min, the solution turned blue-violet owing to the formation of the C_{60}⊂**25** host-guest adduct. Cage **25** was also able to encapsulate C_{70}, however as it was observed for cage **24**, a better fit of C_{60} fullerene inside the cavity resulted in higher association constants than for C_{70}. Unexpectedly, tube **26** showed no affinity towards C_{60} or C_{70} and the authors reasoned that in the case of the analogous tube-like structure **20**, the fullerene⊂receptor interaction was possible due to the presence of Ag-π interactions, whereas those interactions were absent for the Hg(II) analogue.

-insert Figure 13 here-

Figure 13. a) X-Ray crystal structure of the Pd(II)-based molecular capsule 24. **b)** Schematic representation of the C_{60}⊂**24** host-guest adduct.[39] **c**) Mercury(II)-based cage **25** and tube **26** reported by Yoshizawa.[40]

Very recently, the same authors tuned the length of ligand **19** by replacing the phenylene spacer for a naphthalene spacer (Figure 14);[41] the elongated ligand **27** formed a new elliptical cage (**28**) when it was reacted with $[PdCl_2(DMSO)_2]$ and $AgNO_3$ in a 4:2:5 ratio in DMSO, at 100ºC during 2h. The Pd···Pd distance was enlarged from 13.36 Å in cage **24** to 16.1 Å in cage **28**, while the widths of the capsules's cavities where quite similar (~10.3 Å). When cage **28** was suspended in acetonitrile together with C_{70}, a stable 1:1 host-guest adduct was obtained. The anisotropic expansion of the cage enhanced its host capability, and the elliptical shape of the cavity which is complementary to the elliptical form of C_{70} optimized the interaction between the two species.

-insert Figure 14 here-

Figure 14. Chemical formula and schematic representation of ligand **27** (**a**) used for the self-assembly of cage **28** (**b**), reported by Yoshizawa which displays selectivity towards C_{60} fullerene.[41]

First row transition metals, which are attractive from an environmental and economic point of view, have also been used as nexus between pyridine ligands to give cage-like receptors for fullerenes. Würthner used FeX_2 salts (X = BF_4^-, $CF_3SO_3^-$) to link perylene bisimide (PBI) dyes, containing 2,2'-bipyridine groups (**29**), in order to prepare a M_4L_6 tetrahedral structure **30** (Figure 15), which is one of the largest M_4L_6 tetrahedrons ever reported.[42] As a result of the known electronic interaction between C_{60} and the PBI units and considering the large volume of the cage cavity (~950-2150 $Å^3$), nanocapsule **30**

was reacted with an excess of C_{60} (1:10 ratio) in a $CH_3CN/CHCl_3$ mixture (9/1) and the reaction crude was heated to 70ºC overnight. Afterwards the solvents were removed and the remaining mixture was dissolved in CH_3CN and filtered to separate the excess of C_{60} that is insoluble in CH_3CN. The HRMS spectrum displayed peaks corresponding to **30**, $C_{60}\subset$**30** and $2\cdot C_{60}\subset$**30** host-guest adducts (Figure 15b and c). Molecular force field (MMFF) geometry optimization of singly and doubly occupied host-guest complexes indicated that the fullerenes are preferentially located closer to the corners of the tetrahedral cage.[42]

-insert Figure 15 here-

Figure 15. a) PBI-based ligand **29** used in the self-assembly of giant tetrahedral host **30** (**b**) which was able to accommodate one or two molecules of C_{60} fullerene. **c)** ESI-TOF mass spectrum of **30**, $C_{60}\subset$**30** and $2\cdot C_{60}\subset$**30** (CH_3CN). Adapted with permission from (Ref. 42). Copyright (2013) American Chemical Society

Recently, Nitschke reported on the synthesis of a Fe(II)-based M_6L_6 tetragonal cage by self-assembly of diamine 1,6-pyrene-based ligands (6 equiv.) with 2-formylpyridine (12 equiv.) and iron(II)triflimide (4 equiv.). It was found that the resulting cage product consisted of a mixture of three diastereoisomers.[43] Interestingly, both fullerenes C_{60} and C_{70} were observed to form 1:1 host guest adducts with the tetrahedral cage, moreover the cage was able to adapt its structure when binding the fullerene, favouring the formation of the diastereoisomers best able to encapsulate the fullerene in order to maximize the cage-fullerene interaction.

A different strategy was used by Fujita and co-workers who, in the context of metal-organic frameworks (MOFs), developed crystalline sponges for fullerene encapsulation. Previously, the same authors had reported on the synthesis of multiple positively charged nano-vessels by self-assembly of rigid tridentate pyridine ligands through coordination with palladium(II) and platinum(II) (Figure 16a). The corresponding M_6L_4 octahedral flasks were proven to be able to create an isolated micro-environment with properties different from those in the bulk solution and allow small organic molecules to be confined. The authors reported in 2010 on the synthesis of a crystalline coordination network, **32**, generated from an infinite array of octahedral M_6L_4 cages (M= $Co(NCS)_2$), $\mathbf{32_a}$, in which each metal corner is shared between two adjacent octahedra (Figure 16b and c).[44] The cage framework $\mathbf{32_a}$ resembles the octahedral cages previously reported with palladium(II) and platinum(II) ions (**31**, Figure 16a). The crystalline structure of

the MOF revealed the presence of other types of cavities besides the M_6L_4 octahedral cage motifs. The interstitial void spaces between **32_a** moieties (63% of the total lattice volume), define alternating $M_{12}L_8$ (**32_b**) and $M_{12}L_{24}$ (**32_c**) cuboctahedral molecular cages, that are analogous to the palladium(II)-based discrete nanocapsules previously reported. Thus, crystalline infinite network **32** provides three distinct molecular cage environments (**32_{a-c}**).

-insert Figure 16 here-

Figure 16. a) Octahedral coordination Pd(II)- or Pt(II)-based capsules (**31**) reported by Fujita. **b)** Representation of the crystal structures of the three distinct polyhedral molecular cages in the infinite crystalline network **32**. **c)** Inclusion of C_{60} into the crystalline sponge **32,** and photographs of complex **32** before (yellow) and after (black) inclusion of C_{60}. Adapted by permission from Macmillan Publishers Ltd: [Nature Chemistry] (Ref. 44), copyright (2010).

The octahedral cage **32_a** has a narrow window which allows the binding of small organic guests, i.e. tetrathiafulvalene (TTF), through solid-liquid host-guest recognition. On the other hand, the larger cuboctahedra **32_{b-c}** are of an ideal size for the encapsulation of large aromatic guests such as fullerenes. To perform the encapsulation of fullerenes, a crystalline sample of MOF **32** was soaked in C_{60} fullerene containing toluene at 60ºC for a week. During this time the yellow crystals of **32** turned black (Figure 16c). X-ray data was obtained for the inclusion compound and it was found that 35 wt% C_{60} fullerene was accommodated. An analogous experiment was performed using C_{70} and 34 wt% C_{70} was accommodated. The half-lives of the inclusion complexes $C_{60}\subset$**32** and $C_{70}\subset$**32** in toluene were found to be 15 and 25 days respectively. Cages **32_{b-c}** displayed preferential encapsulation towards C_{70} than for C_{60} (C_{60}/C_{70}, 8/2 ratio). The cuboctahedral cages were also used to encapsulate fullerene soot (containing ~7% of fullerenes), where interestingly the C_{70} content was enriched from C_{60}/C_{70}=90/10 to C_{60}/C_{70}=76/24. Moreover, the cuboctahedral cages also showed preferential encapsulation of higher fullerenes from fullerene soot (C_{76}, C_{78}, C_{82} and C_{84}). The content of higher fullerenes relative to C_{60} increased ~3 times upon inclusion.

In the same year, Fujita also reported the synthesis of sphere-like molecular nanocapsules able to isolate fullerenes. The nanosphere **34** was synthesised by self-assembly of ligand **33** treated with $Pd(NO_3)_2$ in DMSO for 4h at 70ºC, resulting in a $M_{12}L_{24}$ cage (Figure 17). The sphere **34** contains 24 large aromatic coronene molecules concentrated inside, which behave as a "nanodroplet" able to host C_{60}. Confined $C_{60}\subset$**34**

in DMSO is 30 times more soluble than in toluene.[45]

-insert Figure 17 here-

Figure 17. Self-assembly of $M_{12}L_{24}$ coordination sphere **34**, using $Pd(NO)_3$ and pendant coronene molecule **34** as molecular building blocks. Adapted with permission from (Ref. 45). Copyright (2010) American Chemical Society.

3.2 Metalloporphyrin-based coordination capsules.

It has been shown that when covalent-multiporphyrinc hosts are used to entrap fullerenes in solution, the association constants dramatically increases compared with the acyclic analogues. However, the covalent synthesis of these receptors is tedious, synthetically complex and often low yielding. Moreover, highly rigid structures are usually formed which in some cases can be detrimental for the host-guest interaction.[23] On the other hand, dimeric porphyrin hosts linked by hydrogen-bonds have also been reported in the literature, but the K_a values observed are usually smaller than those of their covalent analogues.[51] With these precedents, metal-ligand coordination receptors bearing porphyrins appear to be a promising alternative.

In this line Schmittel reported in 2008 the synthesis of an heteroleptic structure ($M_6L_2L'_3$) prepared by self-assembly through copper(I) ions (Figure 18). The reaction between $[Cu(CH_3CN)_4]PF_6$, and ligands **35** (L) and **36** (L'), gave nanocapsule **37** which contains three zinc(II)-porphyrin units, along with some undesired oligomeric aggregates. Subsequent addition of C_{60} to the product mixture provided an extra driving force which shifted the reaction equilibrium towards complete formation of the desired 3D nanocapsule, which contained the fullerene within its cavity ($C_{60}\subset$**37**).[33] In this example, fullerene C_{60} is not just a guest molecule but it also acts as a template leading to a more stable host-guest complex and avoiding the formation of the undesired oligomers. Interestingly, the encapsulation of C_{60} into nanocapsule **37** leads to atypical protons shifts and splitting in the ^{1}H-NMR spectrum. These changes were rationalized by a lateral distortion of the host, resembling an accordion, in order to maximize its interaction with the substrate molecule, leading to a constricted prism which strongly interacts with the fullerene (adaptive structure).

-insert Figure 18 here-

Figure 18. **a**) Ligands **35** and **36** used for **b**) the self-assembly of capsule **37**, which encapsulates C_{60} through its adaptive structure.[33]

A similar strategy was used by Shionoya who reported another example of a metallocage in which the C_{60} fullerene acts as a template molecule, and helps to stabilize the desired product (Figure 19).[46] To perform the metal-ligand directed self-assembly reaction the authors selected zinc(II), a metal centre with a versatile coordination sphere. Despite the variety of geometries that zinc(II) can adopt, by using coordinating anions and solvent molecules, and a proper template molecule (C_{60}), the authors were able to synthesize a discrete tetra-porphyrin structure ($[M_8L_4X_{16}]^{n+}$ X = solvent molecule or *p*-$CH_3C_6H_4SO_3^-$ (**38**)). Initially, the synthesis of cage **39** was attempted by mixing 4 equivalents of *tetrakis*-(bispyridyl)-porphyrin and 8 equivalents of Zn(*p*-$CH_3C_6H_4SO_3)_2$, in a 1:1 mixture of $CHCl_3$/MeOH. However, the major product of this reaction was a porphyrin trimer $[M_8(\mathbf{38})_3X_{12}]^{n+}$, which was in equilibrium with the desired porphyrin tetramer $[M_8(\mathbf{38})_4X_{16}]^{n+}$ (**39**). Finally, it was found that the addition of C_{60} was necessary to shift the equilibrium towards the formation of the $C_{60}\subset$**39** adduct (75%). Single crystal X-ray diffraction analysis confirmed that $C_{60}\subset$**39** was formed by four zinc(II) porphyrins wrapping around a single C_{60} molecule. The tetrameric barrel **39** was not formed when weakly-coordinating anions were used (*i.e.* Zn($CF_3SO_3)_2$). These results indicated that the *p*-$CH_3C_6H_4SO_3^-$ anions play a key role as capping ligands. Thus *p*-$CH_3C_6H_4SO_3^-$ molecules are able to modulate the coordination sphere of the zinc(II) anions and they control the self-assembly interaction between the metal ion and the ligands.

-insert Figure 19 here-

Figure 19. a) Building blocks used for the zinc(II) mediated self-assembly of porphyrin barrel complex $C_{60}\subset$**39**. **b)** X-ray crystal structure of complex $C_{60}\subset$**39** (hydrogen atoms are omitted for clarity).[46]

Another example was reported by Nitschke in 2011 who synthesized a closed-face cubic metallo-cage containing six porphyrin units, which allowed for the isolation of the guest molecules from the bulk solution.[47] In this work the self-assembly reaction was exclusively controlled by the metal ions (iron(II)) and the geometry of the selected pyridine-based ligands. Cage **40** was obtained by reacting nickel(II) *tetrakis*-(4-aminophenyl)porphyrin, 2-formylpyridine and Fe($CF_3SO_3)_2$ in dimethylformamide (DMF) (Figure 20). The cage was obtained as a single product which was confirmed by NMR spectroscopy and ESI-MS. Crystals suitable for X-Ray diffraction were obtained

and the crystallographic data revealed the cage to have an octahedral geometry, containing six porphyrins on its faces and eight iron(II) centres located at the corners (M_8L_6). The volume of the inner cavity was 1340 $Å^3$, large enough to host large aromatic guests such as fullerenes.

-insert Figure 20 here-

Figure 20. Schematic representation of the synthesis of cubic cage **40** through component self-assembly and its X-ray structure (hydrogens and anions are omitted for clarity).[47]

The potential of cage **40** to encapsulate fullerenes was first explored with C_{60}. Cage **40** and C_{60} (5eq.) were mixed in DMF and the reaction was then heated at 70ºC for 5 days. The reaction resulted in a 35% conversion to $C_{60}\subset$**40** adduct ($K_a = 5.5 \cdot 10^3$ M^{-1}). In a subsequent experiment 2 equivalents of C_{70} were added to a solution of the cage in DMF and full conversion to $C_{70}\subset$**40** adduct was obtained after stirring the reaction mixture for 3h at 70ºC. These experiments showed a higher affinity of **40** for C_{70} than for C_{60}, which can be rationalized by the larger surface of the former which facilitates a larger number of stabilizing π-π interactions (Figure 20). To further investigate these findings, an experiment in which 2 equivalents of C_{70} were added to a $C_{60}\subset$**40** solution, resulted in complete conversion towards $C_{70}\subset$**40** as confirmed by ESI-MS. Nanocapsule **40** was then mixed with fullerene soot (C_{60} 53%, C_{70} 1.54%, higher fullerenes 0.14%), in a 1:10 weight ratio and after stirring the mixture for 12 h at 70ºC, neither **40** nor $C_{60}\subset$**40** compounds were observed in the ESI-MS spectrum. However, host-guest adducts with C_{70}, C_{76}, C_{78}, C_{82} and C_{84} fullerenes were observed. Although mass spectra are unable to provide quantitative information, comparable mass ionization behaviour was found for **40** and its fullerene adducts. Therefore from the ESI-MS experiments it was concluded that cage **40** displayed a higher affinity towards higher fullerenes.

Very recently, García-Simón et al reported the synthesis of a tetragonal prismatic coordination cage (**42**), built by metal-directed self-assembly of two tetra-carboxylated Zn(II) porphyrins and four dipalladium(II)-based macrocyclic synthons Pd-**41** (Figure 21).[48] The coordination nanocapsule **42** was fully characterized by NMR, HRMS and UV-Vis spectroscopy. Moreover, crystallographic data for the cationic form of the capsule was obtained by synchrotron X-ray resolution (Figure 22).

-insert Figure 21 here-

Figure 21. Building blocks (**a**) used for the self- assembly (**b**) of the coordination nanocapsule **42** (BArF = tetrakis[3,5-bis(trifluoromethyl)phenyl]borate).[48]

The large void volume of the cage cavity (~696 Å) prompted the authors to explore the possibility to encapsulate fullerene molecules. Delightfully, fast inclusion of C_{60} and C_{70} fullerenes occurred during the mixing of a solution of capsule **42** in acetonitrile and the corresponding fullerene in toluene, in a 1:1 molar ratio. The data obtained from the UV-vis and fluorescence titration experiments indicated that the capsule presents high affinity towards C_{60} and C_{70} fullerenes, K_a (C_{60}) ~$3 \cdot 10^{-7}$ M^{-1} and K_a (C_{70}) ~$4 \cdot 10^{-8}$ M^{-1}. Structural data for the $C_{60}\subset$**42** and $C_{70}\subset$**42** was also obtained by synchrotron radiation. Interestingly, comparison of the crystallographic data of the empty capsule **42**, $C_{60}\subset$**42** and $C_{70}\subset$**42** adducts showed that the distance between the two Zn(II) porphyrins is maximized when guest molecules are absent. Indeed, the distance is compressed upon inclusion of C_{70} or C_{60} (Figure 22). This experimental trend that was confirmed by *state-of-the-art* DFT calculations indicated that the cage has de ability to adapt its structure upon guest encapsulation (breathing ability). This experimental results encouraged the authors to explore the possibility of encapsulating a bulkier [60]PCBM derivate and higher fullerene C_{84}. NMR, UV-Vis and HRMS experiments indicated that 1:1 host-guest adducts were obtained with both substrates. Fast inclusion was also observed when fullerene mixtures, fullerene extract (C_{60} 70%, C_{70} 28%, higher fullerenes 2%) or fullerene soot (C_{60} 53%, C_{70} 1.54%, higher fullerenes 0.14%), were used. Host guest adducts with the more abundant C_{60} and C_{70} fullerenes were observed, as well as inclusion compounds of higher fullerenes such us C_{76}, C_{78} and C_{84}. More interestingly, the encapsulation of the fullerenes can be performed by only soaking a sample of the solid capsule in fullerene containing toluene. When the solid nanocapsule was suspended in a toluene solution of C_{60} or C_{70} and after stirring for 5-10 minutes at room temperature, full encapsulation was confirmed by HRMS. The same results were obtained for a solution of fullerene extract in toluene. This solid-liquid encapsulation strategy is similar to the one reported by Fujita in which a MOF crystal was used to catch fullerenes (Figure 16). The solid-liquid encapsulation of fullerenes within capsule **42**, supports the idea that the fullerenes enter the nanocapsule through one of the four lateral apertures of the capsule, which are large enough to allow easy mobility of the fullerenes through them.

-insert Figure 22 here-

Figure 22. Crystallographic data for cationic capsule **42** (left) and it corresponding fullerene inclusion compounds C_{70}⊂**42** (middle) and C_{60}⊂**42** (right). In all structures hydrogens have been omitted for clarity.[48]

4. Release of the sequestered fullerene molecules.

As it has been mentioned in this review article, there are key factors to consider when designing a molecular receptor for binding fullerenes, such as the fullerene-receptor complementarity and the receptor tunability. However, from a practical point of view it is indispensable to design a system capable of liberating the sequestered fullerenes in an efficient manner, for the selective delivery or utilization of the captured fullerenes. The controllable binding-release of the fullerene would allow to obtain reusable receptors and to recover the fullerene molecule. Therefore, reversibility is envisioned as the key to obtain sustainable purification of fullerene molecules by using molecular host platforms. Usually, the liberation of fullerene causes irreversible cage disassembly or the receptor is blocked by a high-affinity secondary guest.[24] For these reasons the use of host-guest systems as means of separating mixtures of fullerenes remains as a challenging task. Nevertheless, there are few methods described in the literature in which the liberation of the fullerene from the receptor has been achieved, and the host platforms have been recovered, in some cases with excellent yields. Examples of controlled fullerene release will be discussed in this last section.

4.1. Covalent systems

Covalent receptors generally have a more robust structure than receptors based on supramolecular interactions. Consequently, harsh methodologies such as high temperatures or acidic conditions can be applied in order to release the entrapped fullerene without causing host decomposition.

By using CTV-based dimeric capsule **1** (Figure 1), Chiu and co-workers were able to selectively encapsulate C_{70} fullerene from a mixture of fullerenes (Figure 23a).[16] Taking advantage of the higher affinity towards C_{70}, the authors designed an experimental protocol to isolate C_{70} from fullerene extract. The separation process consists in 3 main steps: 1) Formation of the C_{70}⊂**1** complex. First the molecular host **1** and the fullerene extract were mixed in a TCE solution (in a 1/6-cage/extract weight ratio), the remaining solution was heated at 313 K during 16h; afterwards, the TCE was removed by

evaporation and the remaining solid was re-dissolved in DCM and the resulting solution was filtered in order to remove the fullerenes in excess. 2) Isolation of C_{70}⊂**1** adduct. The filtrate was concentrated and introduced in a short SiO_2 column, and eluted with CS_2 in order to further remove any uncomplexed or dissociated fullerene. Free host **1** and its corresponding C_{70}⊂**1** adduct were recovered from the chromatographic column using DCM/Hexane and DCM/MeOH as mobile phases. 3) Liberation of the C_{70}. Finally, the filtrate from the SiO_2 column was dried and the product re-dissolved in toluene. The toluene solution was heated up to 303 K during 12h. The host **1** precipitated from the solution as a white solid while the liberated C_{70} and residual C_{70}⊂**1** complex remained in solution. Isolated C_{70} was separated from the residual host-guest complex by centrifugation. The purity of the isolated C_{70}, determined through HPLC analysis was ~99%. After the first liberation cycle ~85% of receptor **1** was recovered, and it was used in a second cycle without further purification. The dissociation of C_{70} from recycled **1**, following the same experimental protocol, gave C_{70} with ~92% purity. To our knowledge, the amount of receptor **1** recovered from the second liberation cycle was not reported.

A different strategy was followed by Zhang, who demonstrated that receptor **4** (Figure 2) presents a much higher association constant for C_{70}than for C_{60} ($K_a(C_{70})/K_a(C_{60})>1000$).[18] Considering the difference in binding affinity the authors worked on the controlled selective separation of C_{70} from fullerene mixtures. The porphyrin-fullerene interaction could be easily tuned just by protonation of the non-metallated porphyrin. The protonation of the porphyrin reduces its electron-donating ability, and thus the porphyrin-fullerene interaction is weakened. Therefore, the fullerene association-dissociation was reversible and controlled by changing the pH of the media (Figure 23b). The authors optimized the isolation process in three steps: 1) the cage is added to a C_{60}/C_{70} (91% C_{60} and 9% C_{70}) solution in CS_2, and sonicated for 30 seconds; 2) then the host-guest adducts are collected in a chloroform solution, whereby upon addition of 100 equivalents of trifluoroacetic acid (TFA) to the chloroform solution, the fullerene molecules (mainly C_{70}) are released as a black precipitate and removed. Once a cycle of the isolation process was completed, the abundance of C_{70} in the sample increased from 9 mol% to 79 mol%. 3) in a final step the nanocapsule was recovered by the addition of 100 equivalents of triethylamine (TEA) to the remaining chloroform solution. Remarkably, the efficiency of the protocol was demonstrated by UV-Vis

experiments. The regeneration of the C_{70}⊂**4** adduct by the addition of 100 eq. of TEA to the mixture of protonated recycled **4** and free C_{70} was evidenced by a UV-Vis band that was almost identical than the one belonging to the initial pure C_{70}⊂**4** complex. The observation of an almost identical UV-vis spectra indicated that nearly all the cage can be recovered after fullerene liberation; the cycle was repeated up to 5 times.

-insert Figure 23 here-

Figure 23. Reported strategies for fullerene release from covalent molecular receptors. (**a**) Prolonged heating to cause the precipitation of the host.[16] (**b**) Protonation and deprotonation of the porphyrin.[18]

4.2. Supramolecular receptors

Despite of the fact that covalent receptors for fullerenes allow for their reversible encapsulation, generally the experimental protocols required to recover the fullerenes and the receptors are quite tedious (section 4.1). In the case of supramolecular receptors, these can easily change their conformation, geometry (especially in the case of coordination capsules), and even molecular structure, commonly in a reversible fashion. This greater versatility (tunable capsule geometry, electronic and symmetry) facilitates the liberation of the entrapped fullerenes.

4.2.1. Hydrogen bonded systems

Mendoza and co-workers also used TFA to disassemble host **13** (Figure 7 and Figure 24a).[30] In this case the addition of the acidic solution caused the hydrogen-bonded network to break and the fullerenes to precipitate. The fullerene extraction experiments were performed in tetrahydrofuran (THF), since receptor **13** is highly soluble in this solvent, while the corresponding solubility of the fullerenes is very limited. Again taking advantage of the differences in the binding of C_{60} and C_{70} within **13**, the authors designed an experimental setup to extract C_{70} from fullerene extract (with a C_{60}/C_{70} ratio of ~ 79/21). The experimental protocol consisted in two main steps: 1) To a solution of the cage in THF, fullerenes were added in the solid state and stirred for 15 minutes at room temperature, fullerene⊂**13** adducts were formed; afterwards the fullerenes in excess remaining as a solid were removed from the solution by filtration, and the clean filtrate was analysed by reverse phase HPLC. The first extraction cycle yielded mixtures notably enriched with C_{70} (C_{60}/C_{70} ratio of 16/84). In step 2) fullerene

release from the capsule was achieved by addition of TFA, which caused the precipitation of the fullerenes from the mixture and the cage remaining in the THF solution was recovered by evaporation. In the second extraction cycle the C_{60}/C_{70} ratio was further improved to 3/97. Interestingly, higher fullerenes (from C_{76} to C_{84}) were also extracted, most likely due to the flexible structure of the capsule, and the sample of fullerenes was enriched over its initial content of higher fullerenes (initial ratio of higher fullerene in the extract <2%).

-insert Figure 24 here-

Figure 24. Reported strategies for fullerene release from supramolecular capsules. (**a**) Acid or basic treatment to provoke a structural rearrangement of the host.[30] (**b**) Photoreduction of metal ions to disassemble metal-coordination-based supramolecular host.[36] (**c**) Transformation of the shape of the cage in response to an external stimulus.[40] (f) solid-liquid solvent washing strategy.[48]

4.2.2. Coordination receptors

There are two main advantages of coordination fullerene receptors with respect to other supramolecular or covalent structures. On one hand they can easily interconvert their geometry due to the fact that metal ions used as nexus in the structure can often exhibit multiple coordination modes. This structural interconversion can be easily controlled by external stimulus as it will be explained henceforth. On the other hand metal-based structures are highly dynamic and flexible, which may also facilitate the liberation of fullerenes.

4.2.2.1. Transformable cages

Strikingly, Yoshizawa and co-workers were able to release C_{60} from their tubular receptor **20** by using light as a non-invasive stimulus (Figure 10 and 22 b).[36] Interestingly, when a red-purple solution containing $C_{60}\subset$**2** was irradiated with a 36W incandescent light (UV-vis irradiation, acetonitrile, room temperature, 1.5h) the solution turned yellow and a precipitate corresponding to C_{60} and metallic silver appeared. The released C_{60} was extracted with toluene and recovered as a brown solid (68%). Finally, UV-vis irradiation of the remaining yellow solution containing ligand **19** in the presence of C_{60} and $AgNO_3$, allowed recovery of the host-guest adduct $C_{60}\subset$**20** in ~60% yield. As it has been mentioned, tube **20** displayed better affinity for C_{60} than for C_{70}. Hence, when it was used to encapsulate fullerenes from commercially available fullerene soot containing only 5% of C_{60}, the designed catch-and-release procedure provided pure C_{60}

in 63% yield based on **20**.

The same authors also took advantage of the structural rearrangement strategy to liberate fullerenes from their Hg(II)-based 3D cage (**25**) (Figure 13 and Figure 24 c),[40] since the tube-like receptor **26** displayed no interaction with C_{60} or C_{70} while cage **25** displays affinity for both species. The stronger binding affinity of capsule **25** was ascribed to its greater number of anthracene panels interacting with the fullerene molecule and full enclathration in all the directions. Interestingly, all the fullerenes embedded in cage **25** were quantitatively liberated upon capsule-to-tube conformational transformation induced by the simple addition of metal ions (from **25** to **26**). When 2 equivalents of $Hg(CF_3SO_3)_2$ were added to a blue-violet solution of $C_{60}\subset$**25** in acetonitrile, the solution turned pale yellow, and a brown suspension of C_{60} was formed upon guest expulsion, which was recovered by centrifugation. Hence the conformational change and the fullerene liberation phenomenon could be detected by the naked eye on the basis of the change in colour. The encapsulation and liberation of C_{70} was also successfully performed using the same reaction conditions.

4.2.2.2. Solid washing strategy

Capsule **42** can encapsulate fullerenes when it is soaked as a solid in fullerene containing toluene, leading the authors to envision that a solid washing strategy might be appropriate in order to design a straightforward experimental protocol to release the sequestered fullerenes in a selective fashion (Figure 21 and Figure 24d).[48]

The encapsulation-liberation process was first explored for C_{60} and monitored by HRMS (Figure 25). The designed experimental protocol consists in two main stages: 1) A solid sample of **42** was charged in a small column of Celite®. Then a solution of C_{60} in toluene was passed through the column until full encapsulation was confirmed by HRMS (Figure 25). 2) Afterwards, liberation of C_{60} was achieved by consecutive washings of the solid sample of $C_{60}\subset$**42** retained on the column, with a mixture of 1,2-dichlorobenzene/CS_2 (1/1 v/v mixture). This solvent mixture fulfilled the requirements of both a high solubility for the fullerene and a low solubility for the **42** receptor and $C_{60}\subset$**42** adduct. Washing the solid containing the fullerene five times with the chosen solvent mixture (~1.3 mL/mg), was sufficient to liberate all of the encapsulated C_{60} as confirmed by HRMS. Delightfully, the solid remaining on the column was pure empty capsule **42**, which was ready to be filled again with C_{60} and to repeat the cycle. The

solid-liquid encapsulation-liberation protocol was repeated up to 5 times and finally the capsule which was retained on the column was recovered by dissolving it in acetonitrile. After 5 encapsulation-liberation cycles, 91% of the initial capsule was recovered which makes this strategy very efficient. Note that Fujita's MOF sponge could only liberate fullerenes by deconstruction of the crystals by acid treatment.[44]

The same solid washing strategy allowed to selectively separating C_{60} from fullerene extract (C_{60} 70%, C_{70} 28%, higher fullerenes 2%). However, ineffective mixing in the column between the solid cage sample and the solution containing the mixture of fullerenes, gave inhomogeneous distribution of the later among the solid. The authors therefore decided to perform the encapsulation in solution (capsule in CH_3CN and fullerene extract in toluene were mixed), and the fullerene containing cage was precipitated out by addition of diethyl ether and re-introduced in the column. At the first encapsulation-liberation cycle the ratio of $C_{60}\subset$**42**/ $C_{70}\subset$**42** was 4/1, and exclusively C_{60} was released from the capsule after washing the inclusion compound with a 1:1 mixture of 1,2-dichlorobenzene/CS_2. When the cycle was repeated up to 7 times (~10% mass lost was observed after each cycle), the capsule was enriched of mainly C_{70} and other higher fullerenes. Concerning the recovery of the retained higher fullerenes (mainly C_{70} and C_{84}), different solvent mixtures were tested but no significant liberation was achieved. Deconstruction of the nanocapsule could be then achieved by addition of TFA, releasing C_{70} and other higher fullerenes sequestered within the saturated cage retained in the column. Finally, the capsule could be partially re-constructed by treatment with TEA in DMF under reflux.

-insert Figure 25 here-

Figure 25. a) Images of the experimental protocol used for the solid-liquid encapsulation and liberation of C_{60} fullerene from solid nanocapsule **42** (**I.** Solid capsule retained in the Celite® column, **II.** A solution of C_{60} in toluene is passed through the column, **III.** C_{60} is released by consecutive washing with a 1/1 mixture of 1,2-dichlorobenzene/carbon disulphide and **IV.** Cage recovery by solving it in CH_3CN). b) HRMS monitoring of the C_{60} extraction washing-protocol using pure C_{60} encapsulated within capsule **42** in the solid state.[48]

5. Summary and future prospects.

Fullerenes have potential applications in multiple research fields such as materials science and medicine. However, these applications are limited in origin by the cost of purification of fullerenes. Despite the fact that fullerene extracts are easily available at

macroscopic quantities from fullerene soot, finding an efficient strategy to obtain these molecules in a pure form remains elusive, especially for higher fullerenes (C_n, n>70). Nowadays, efficient chromatographic techniques are available for the purification of fullerenes, but still more sustainable, selective and versatile methodologies are required.

In this Tutorial Review the use of molecular receptors for the separation of fullerenes by means of host-guest interactions has been covered. Some insight has been given about the key factors that need to be considered when designing a fullerene molecular receptor: structural complementarity, electronic complementarity and receptor tunability.

Although very elegant examples of covalent and hydrogen-bonded fullerene hosts have been described on the literature, in this review the attention has been focused on coordination supramolecular receptors. The synthesis of covalent receptors commonly follows tedious and low yielding experimental protocols, whilst in the case of hydrogen-bonded structures the calculated values of the binding constants are low in contrast to the ones achieved with covalent hosts ($K_{H\text{-}bonded}$ ($10^5 M^{-1}$) <<< $K_{Covalent}$ (10^9 M^{-1})). The metal-ligand coordination approach emerged as a promising alternative to solve the synthetic cost of covalent strategies while increasing the association constants of hydrogen-bonded structures. Due to the diversity of organic ligands (linkers) and transition metals available, the metal-ligand coordination approach allows for the generation of a manifold number of supramolecular structures. This approach offers a versatile and controlled strategy to design fullerene receptors due to the predictable metal ion coordination environment, and has tunabilily advantages with respect to MOFs. Moreover, the latter are limited to often slow solid-liquid host-guest reactions. Besides the greater robustness of coordination structures in comparison with other supramolecular structures (i.e. hydrogen bonded receptors), these also present a flexible and dynamic structure which facilitates and improves the interaction with the fullerene molecule. Binding constants up to 10^8 M^{-1} have been achieved by using this approach ($K_{H\text{-}bonded}$~10^5 << $K_{coordination}$ ~10^8 < $K_{covalent}$ ~10^9). Throughout this review the advantages of this approach have been discussed and relevant examples of coordination polygons and cage-like structures able to accommodate fullerenes have been detailed.

In the last part of the review, it has been shown that the efficient recovery of the encapsulated fullerenes is possible, impacting in the practicability of fullerene purification methodologies. Strategies ranging from thermal or acid treatments, to

conformational and structural rearrangements are the most promising ones since the host can be partially recovered. Strikingly, very recently a solid-washing strategy has been described in which fullerene C_{60} can be reversibly encapsulated/released from a coordination capsule (**42**), without the need to disassemble the cage or do any further treatment to recover the recycled host. Moreover the receptor was re-used up to 5 times, and finally > 91% of the capsule was recovered.

The application of molecular receptors for the purification of fullerenes is in its infancy, and still a lot of effort needs to be devoted to the development of new methodologies. Nevertheless, the field is rapidly evolving and more convenient solutions to the current tedious, time- and energy-consuming chromatographic methods might appear in the near future.

6. References

1. H. W. Kroto, J. R. Heath, S. C. O'Brien, R. F. Curl, and R. E. Smalley, *Nature*, 1985, **318**, 162–163.
2. M. Prato, *J. Mater. Chem.*, 1997, **7**, 1097–1109.
3. G. Dennler, M. C. Scharber, and C. J. Brabec, *Adv. Mater.*, 2009, **21**, 1323–1338.
4. Y. Iwasa, *Nature*, 2010, **466**, 191–2.
5. G.-F. Liu, M. Filipović, I. Ivanović-Burmazović, F. Beuerle, P. Witte, and A. Hirsch, *Angew. Chem. Int. Ed.*, 2008, **47**, 3991–4.
6. C. Yeretzian, J. B. Wiley, K. Holczer, T. Su, S. Nguyen, R. B. Kaner, and R. L. Whetten, *J. Phys. Chem.*, 1993, **97**, 10097–10101.
7. M. Hirch, A. and Brettreich, *Fullerenes: chemistry and reactions*, Wiley-VCH, Weinheim, Germany, 2005.
8. D. Canevet, E. M. Pérez, and N. Martín, *Angew. Chem. Int. Ed.*, 2011, **50**, 9248–59.
9. P. D. W. Boyd and C. a Reed, *Acc. Chem. Res.*, 2005, **38**, 235–42.
10. J. Effing, U. Jonas, L. Jullien, T. Plesnivy, H. Ringsdorf, F. Diederich, C. Thilgen, and D. Weinstein, *Angew. Chem. Int. Ed.*, 1992, **31**, 1599–1602.
11. T. Andersson, K. Nilsson, M. Sundahl, G. Westman, and O. Wennerström, *J. Chem. Soc. Chem. Commun.*, 1992, 604.
12. Y. Liu, H. Wang, P. Liang, and H.-Y. Zhang, *Angew. Chem. Int. Ed.*, 2004, **43**, 2690–2694.
13. J. L. Atwood, G. A. Koutsantonis, and C. L. Raston, *Nature*, 1994, **368**, 229–231.
14. Z. Yoshida, H. Takekuma, S. Takekuma, and Y. Matsubara, *Angew. Chem. Int. Ed.*, 1994, **33**, 1597–1599.
15. Y. Nakanishi, H. Omachi, S. Matsuura, Y. Miyata, R. Kitaura, Y. Segawa, K. Itami, and H. Shinohara, *Angew. Chem. Int. Ed.*, 2014, **53**, 3102–6.

16. M.-J. Li, C.-H. Huang, C.-C. Lai, and S.-H. Chiu, *Org. Lett.*, 2012, **14**, 6146–9.

17. M. Ku, S.-J. Huang, S. Huang, Y. Liu, C.-C. Lai, S.-M. Peng, and S.-H. Chiu, *Chem. Commun.* , 2014, **50**, 11709–12.

18. C. Zhang, Q. Wang, H. Long, and W. Zhang, *J. Am. Chem. Soc.*, 2011, **133**, 20995–1001.

19. Y.-B. Wang and Z. Lin, *J. Am. Chem. Soc.*, 2003, **125**, 6072–3.

20. K. Tashiro and T. Aida, *Chem. Soc. Rev.*, 2007, **36**, 189–97.

21. L. P. Hernández-Eguía, E. C. Escudero-Adán, I. C. Pintre, B. Ventura, L. Flamigni, and P. Ballester, *Chem. Eur. J.*, 2011, **17**, 14564–77.

22. G. Gil-Ramírez, S. D. Karlen, A. Shundo, K. Porfyrakis, Y. Ito, G. A. D. Briggs, J. J. L. Morton, and H. L. Anderson, *Org. Lett.*, 2010, **12**, 3544–7.

23. J. Song, N. Aratani, H. Shinokubo, and A. Osuka, *J. Am. Chem. Soc.*, 2010, **132**, 16356–7.

24. K. Tashiro, T. Aida, J.-Y. Zheng, K. Kinbara, K. Saigo, S. Sakamoto, and K. Yamaguchi, *J. Am. Chem. Soc.*, 1999, **121**, 9477–9478.

25. S. S. and K. Y. Jian-Yu Zheng, Kentaro Tashiro, Yusuke Hirabayashi, Kazushi Kinbara, Kazuhiko Saigo, Takuzo Aida, *Angew. Chem. Int. Ed.*, 2001, **40**, 1857–1861.

26. M. Yanagisawa, K. Tashiro, M. Yamasaki, and T. Aida, *J. Am. Chem. Soc.*, 2007, **129**, 11912–3.

27. Y. Shoji, K. Tashiro, and T. Aida, *J. Am. Chem. Soc.*, 2004, **126**, 6570–1.

28. F. Hajjaj, K. Tashiro, H. Nikawa, N. Mizorogi, T. Akasaka, S. Nagase, K. Furukawa, T. Kato, and T. Aida, *J. Am. Chem. Soc.*, 2011, **133**, 9290–2.

29. L. P. Hernández-Eguía, E. C. Escudero-Adán, J. R. Pinzón, L. Echegoyen, and P. Ballester, *J. Org. Chem.*, 2011, **76**, 3258–65.

30. E. Huerta, G. a Metselaar, A. Fragoso, E. Santos, C. Bo, and J. de Mendoza, *Angew. Chem. Int. Ed.*, 2007, **46**, 202–5.

31. E. Huerta, E. Cequier, and J. de Mendoza, *Chem. Commun.* , 2007, 5016–8.

32. T. R. Cook, Y.-R. Zheng, and P. J. Stang, *Chem. Rev.*, 2013, **113**, 734–77.

33. M. Schmittel, B. He, and P. Mal, *Org. Lett.*, 2008, **10**, 2513–6.

34. S. Goeb, S. Bivaud, P. I. Dron, J.-Y. Balandier, M. Chas, and M. Sallé, *Chem. Commun.* , 2012, **48**, 3106–8.

35. S. Shanmugaraju, V. Vajpayee, S. Lee, K. W. Chi, P. J. Stang, and P. S. Mukherjee, *Inorg. Chem.*, 2012, **51**, 4817–4823.

36. N. Kishi, M. Akita, M. Kamiya, S. Hayashi, H. Hsu, and M. Yoshizawa, *J. Am. Chem. Soc.*, 2013, **135**, 12976–9.

37. A. Ikeda, M. Yoshimura, H. Udzu, C. Fukuhara, and S. Shinkai, *J. Am. Chem. Soc.*, 1999, **121**, 4296–4297.

38. I. Sánchez-Molina, B. Grimm, R. M. Krick Calderon, C. G. Claessens, D. M. Guldi, and T. Torres, *J. Am. Chem. Soc.*, 2013, **135**, 10503–11.

39. N. Kishi, Z. Li, K. Yoza, M. Akita, and M. Yoshizawa, *J. Am. Chem. Soc.*, 2011, **133**, 11438–41.

40. N. Kishi, M. Akita, and M. Yoshizawa, *Angew. Chem. Int. Ed.*, 2014, **53**, 3604–7.

41. M. Yamashina, T. Yuki, Y. Sei, M. Akita, and M. Yoshizawa, *Chem. - A Eur. J.*, 2015, **21**, 4200–4204.

42. K. Mahata, P. D. Frischmann, and F. Würthner, *J. Am. Chem. Soc.*, 2013, **135**, 15656–61.

43. T. K. Ronson, A. B. League, L. Gagliardi, C. J. Cramer, and J. R. Nitschke, *J. Am. Chem. Soc.*, 2014, **136**, 15615–24.

44. Y. Inokuma, T. Arai, and M. Fujita, *Nat. Chem.*, 2010, **2**, 780–3.

45. K. Suzuki, K. Takao, S. Sato, and M. Fujita, *J. Am. Chem. Soc.*, 2010, **132**, 2544–5.

46. T. Nakamura, H. Ube, R. Miyake, and M. Shionoya, *J. Am. Chem. Soc.*, 2013, **135**, 18790–3.

47. W. Meng, B. Breiner, K. Rissanen, J. D. Thoburn, J. K. Clegg, and J. R. Nitschke, *Angew. Chem. Int. Ed.*, 2011, **50**, 3479–83.

48. C. García-Simón, M. Garcia-Borràs, L. Gómez, T. Parella, S. Osuna, J. Juanhuix, I. Imaz, D. Maspoch, M. Costas, and X. Ribas, *Nat. Commun.*, 2014, **5**, 5557.

49. A. Ikeda, H. Udzu, M. Yoshimura, and S. Shinkai, *Tetrahedron*, 2000, **56**, 1825–1832.

50. C. G. Claessens and T. Torres, *Chem. Commun.* , 2004, 1298–9.

51. Z. Wu, X. Shao, C. Li, J. Hou, K. Wang, X. Jiang, and Z. Li, *J. Am. Chem. Soc.*, 2005, **127**, 17460–8.

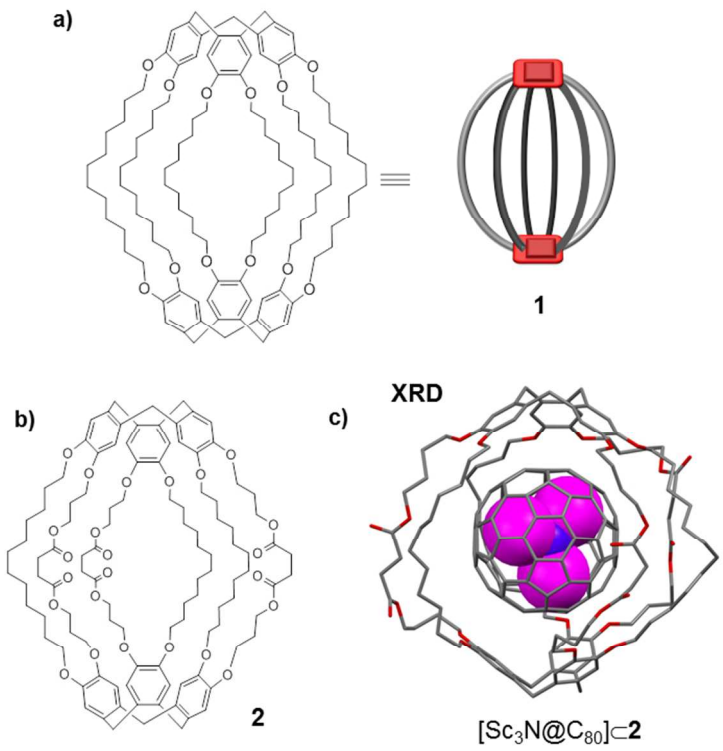

254x190mm (96 x 96 DPI)

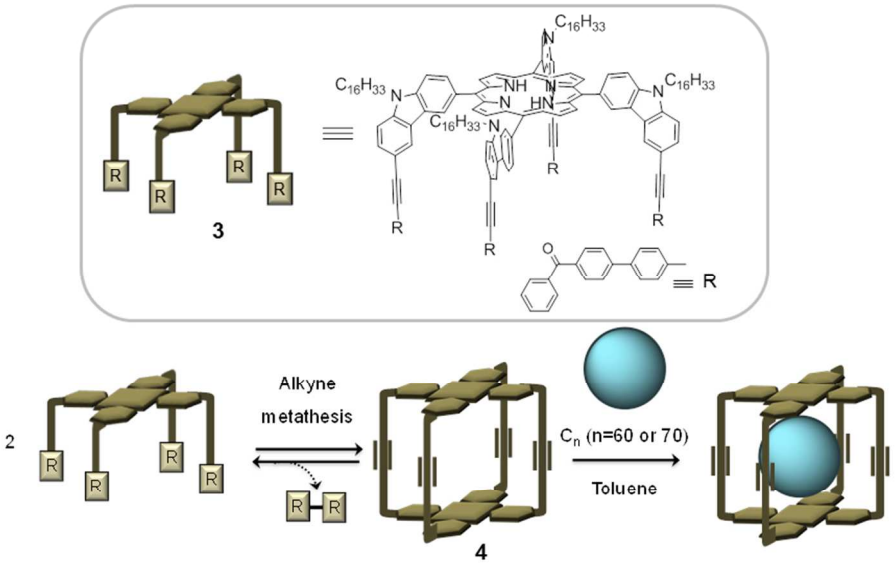

254x190mm (96 x 96 DPI)

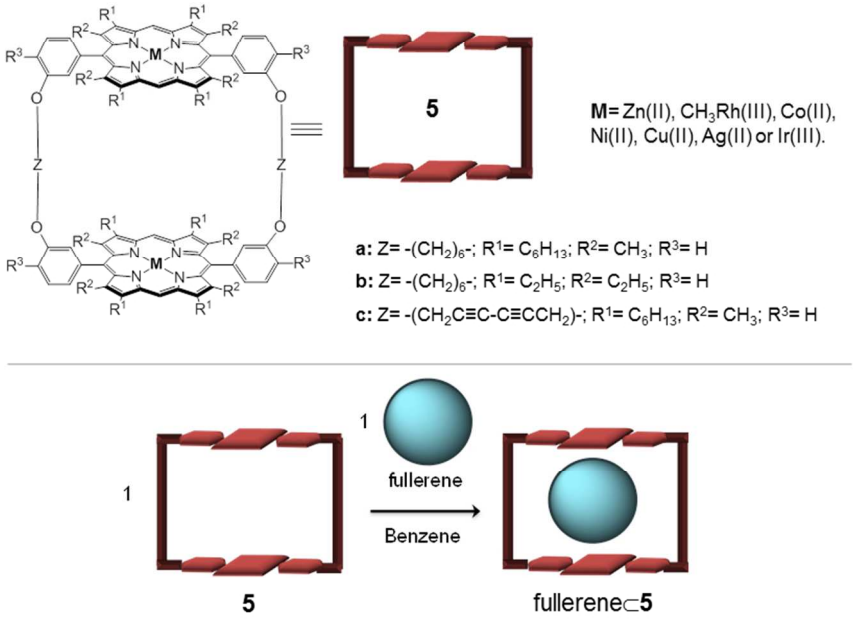

254x190mm (96 x 96 DPI)

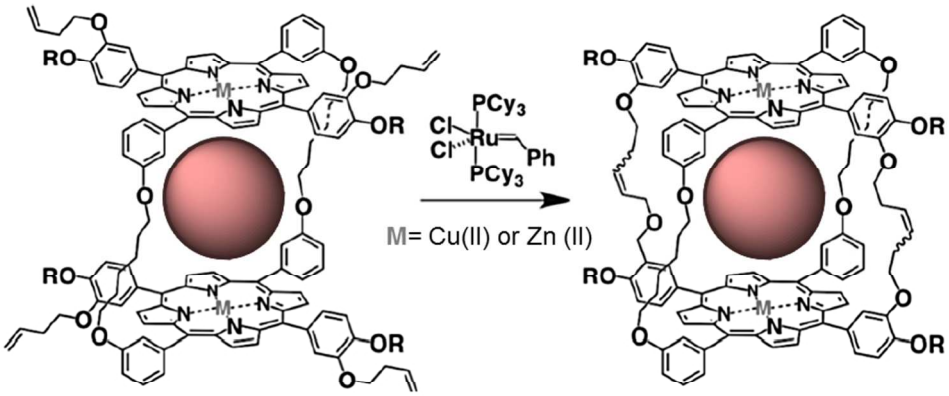

[La@C_{82}⊂**6**$_{cyclo}$] [La@C_{82}⊂**6**$_{cage}$]

254x190mm (96 x 96 DPI)

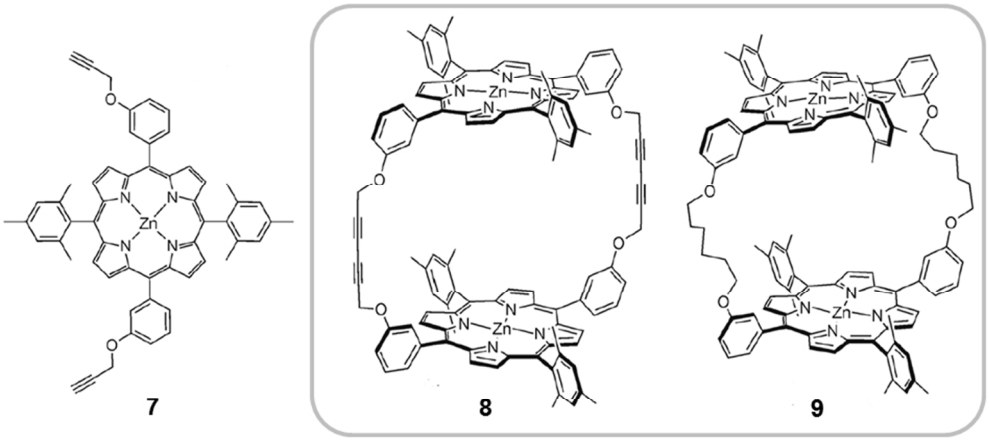

254x190mm (96 x 96 DPI)

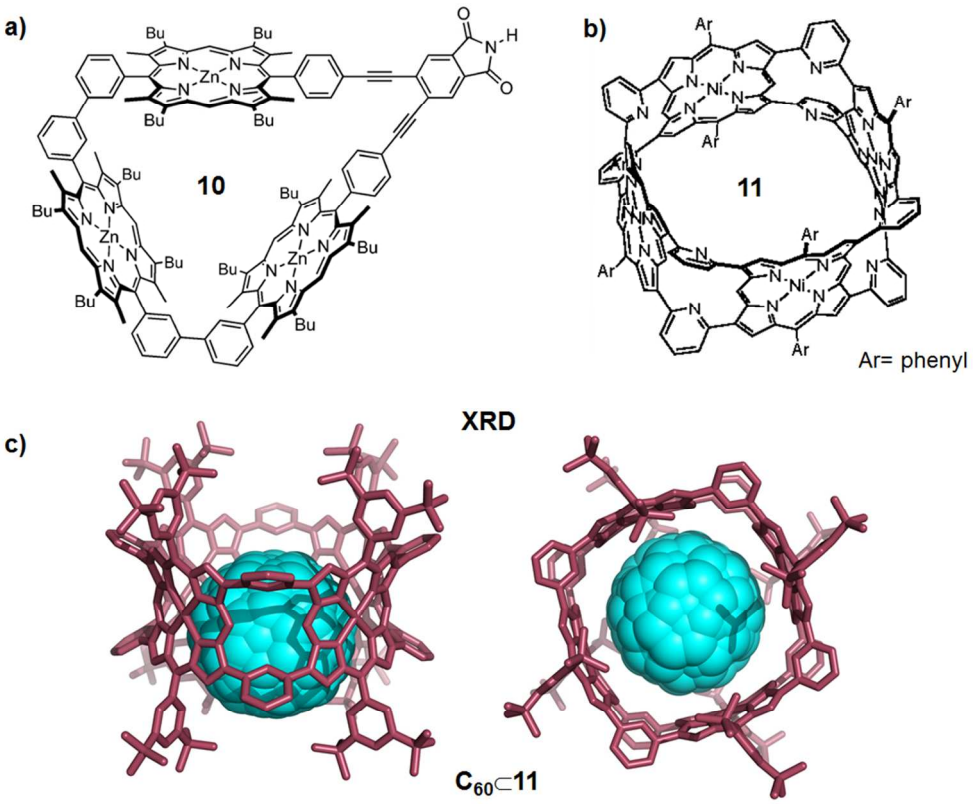

286x231mm (96 x 96 DPI)

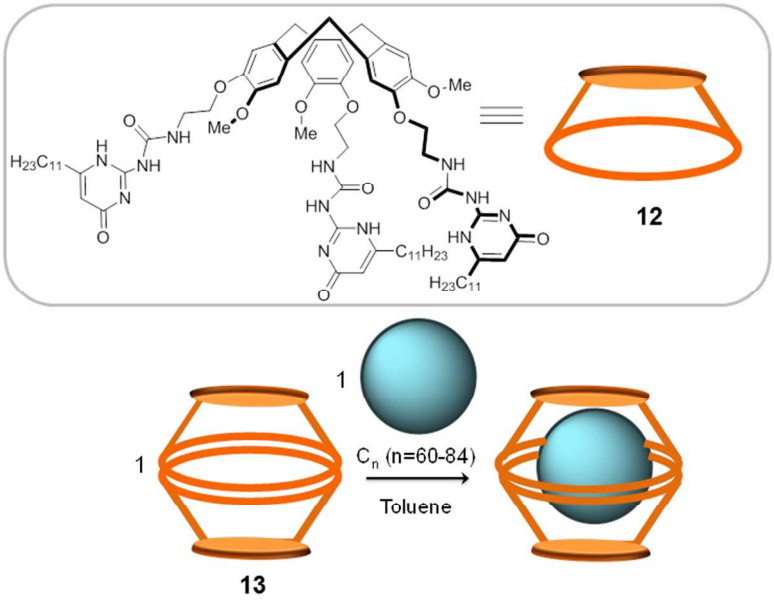

254x190mm (96 x 96 DPI)

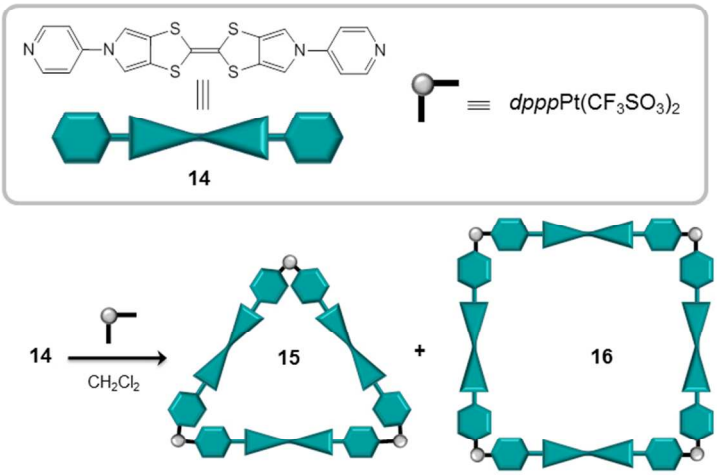

254x190mm (96 x 96 DPI)

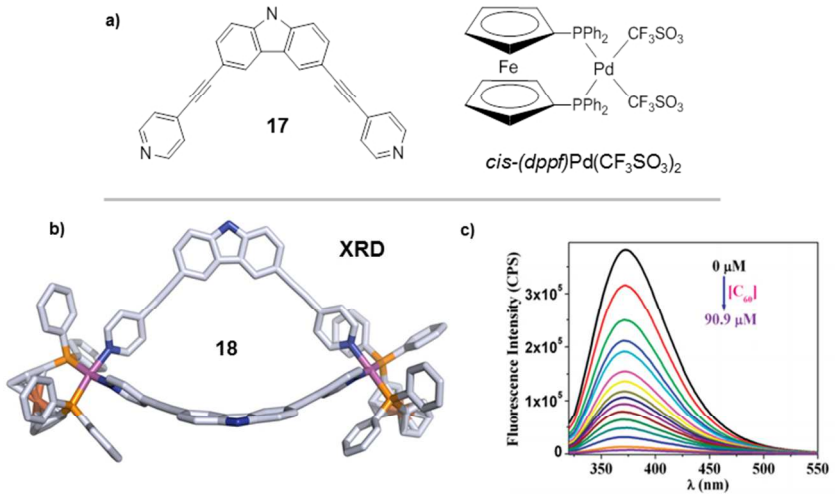

254x190mm (96 x 96 DPI)

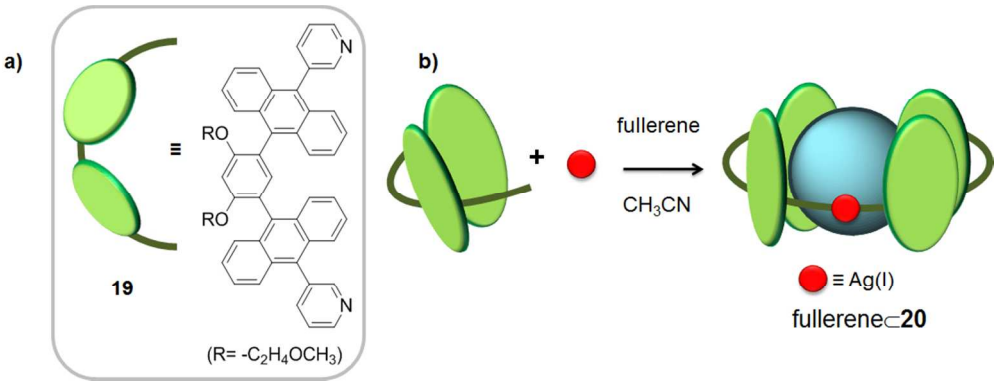

298x112mm (96 x 96 DPI)

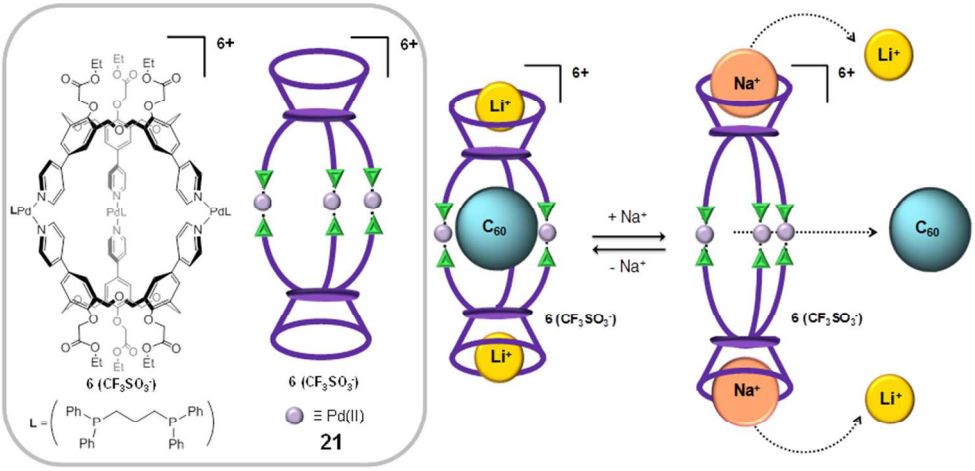

254x190mm (96 x 96 DPI)

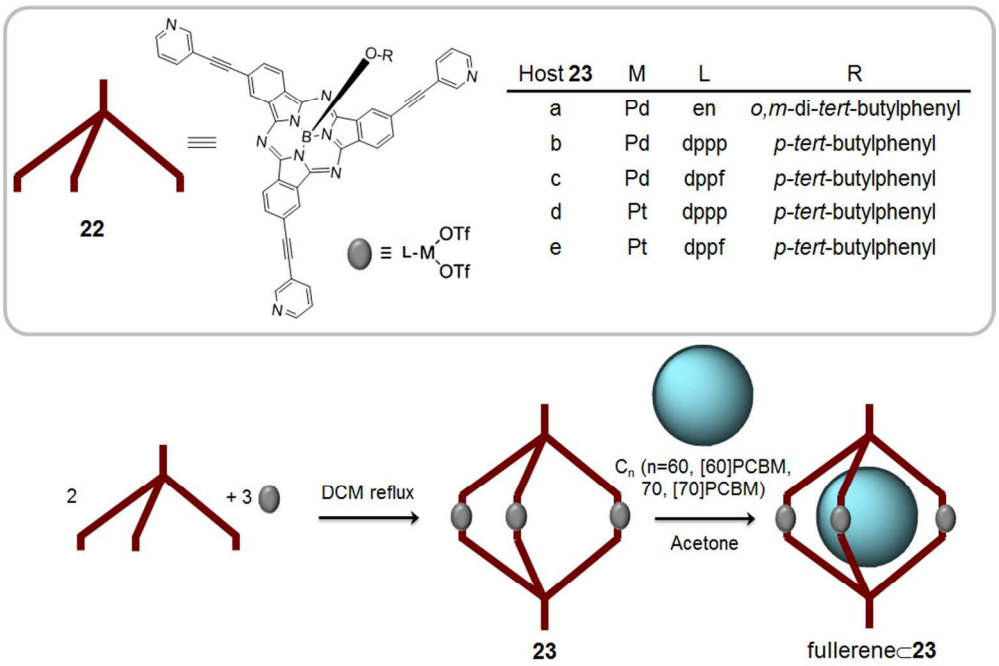

Host **23**	M	L	R
a	Pd	en	*o,m*-di-*tert*-butylphenyl
b	Pd	dppp	*p*-*tert*-butylphenyl
c	Pd	dppf	*p*-*tert*-butylphenyl
d	Pt	dppp	*p*-*tert*-butylphenyl
e	Pt	dppf	*p*-*tert*-butylphenyl

279x188mm (96 x 96 DPI)

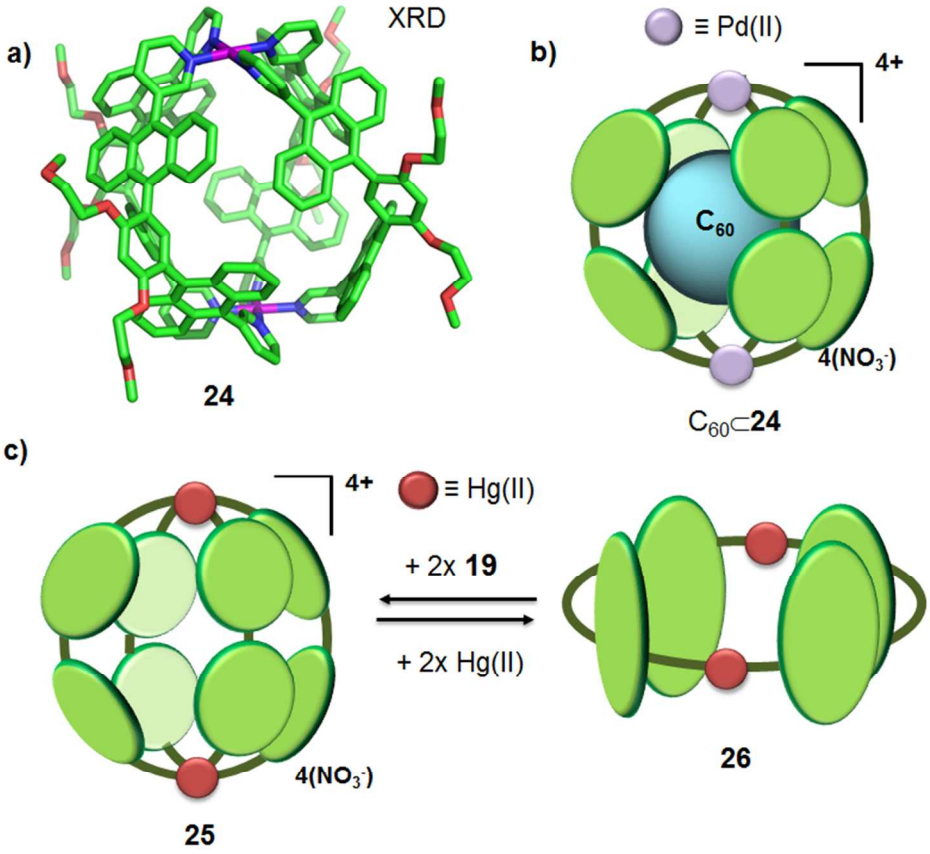

222x196mm (96 x 96 DPI)

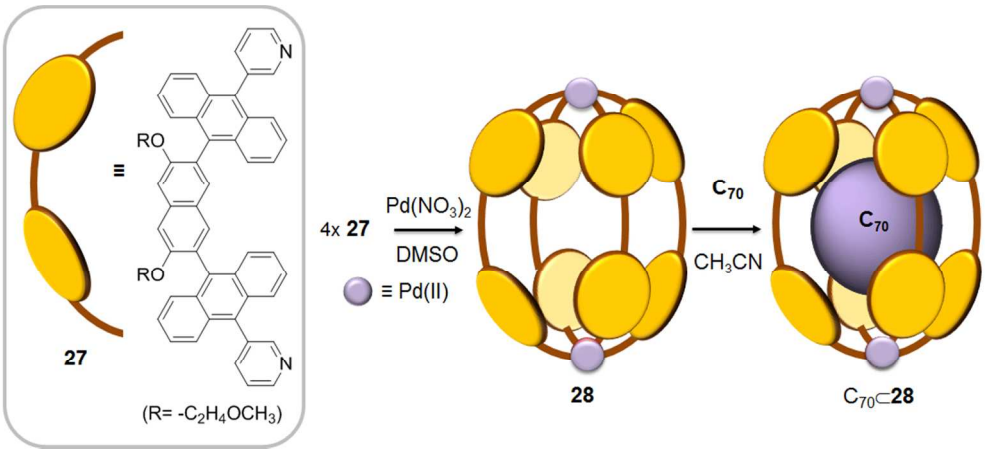

290x128mm (96 x 96 DPI)

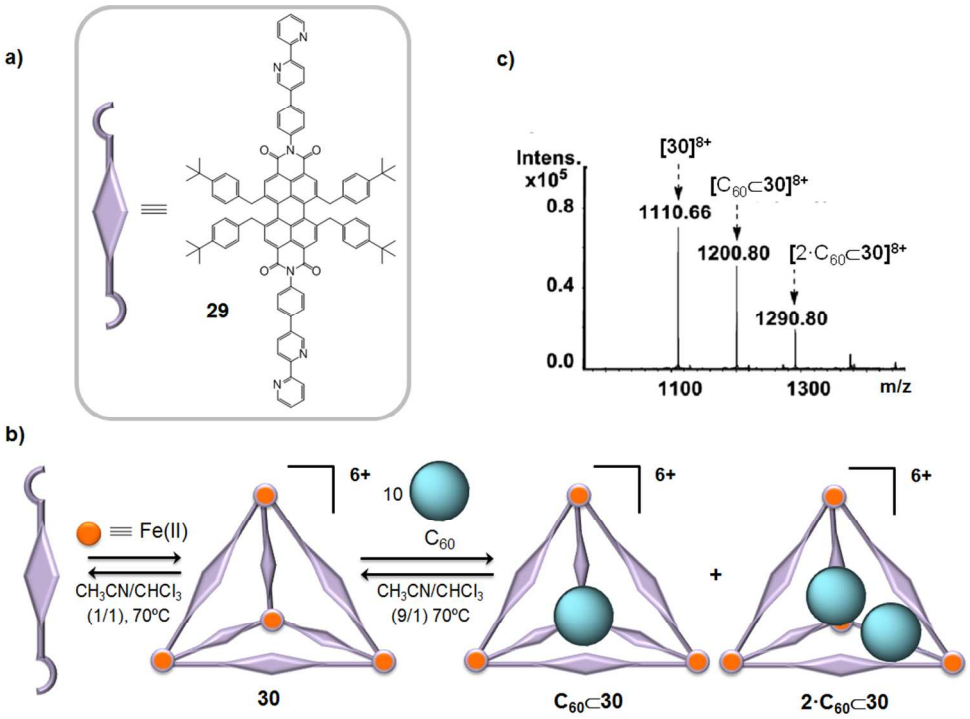

301x216mm (96 x 96 DPI)

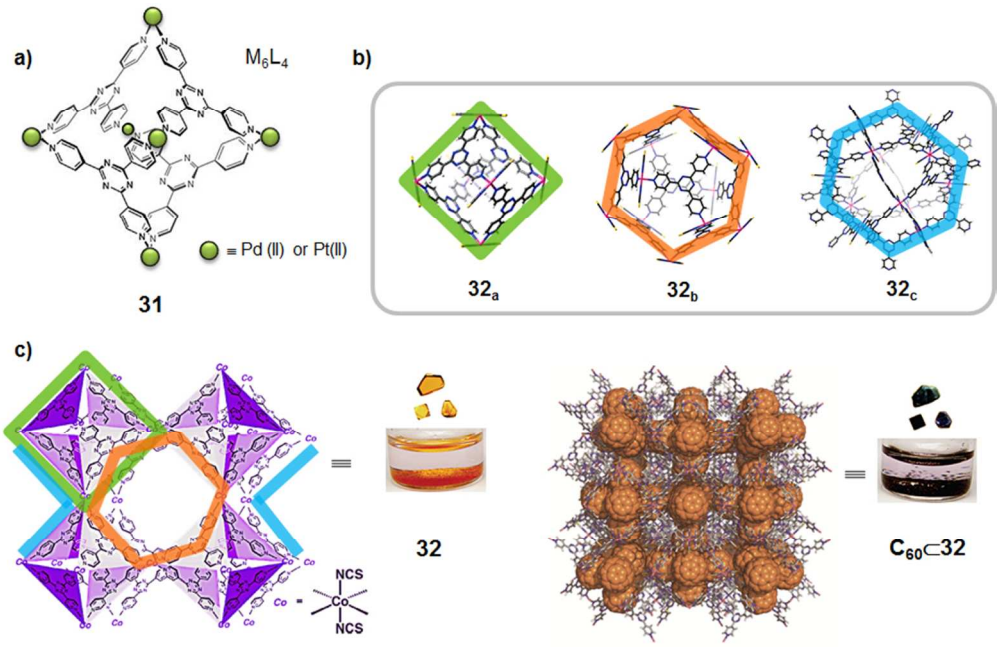

244x157mm (96 x 96 DPI)

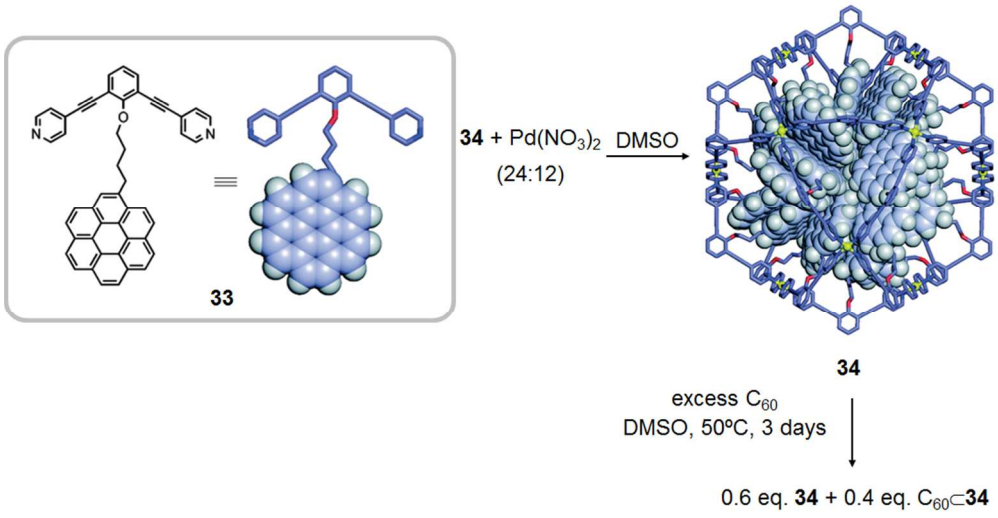

288x152mm (96 x 96 DPI)

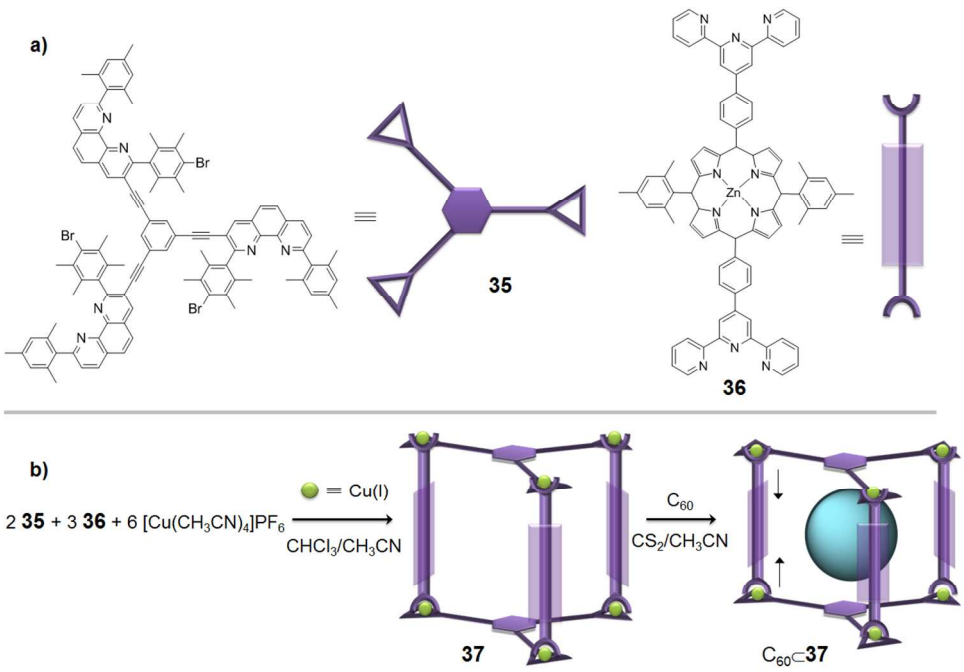

360x242mm (96 x 96 DPI)

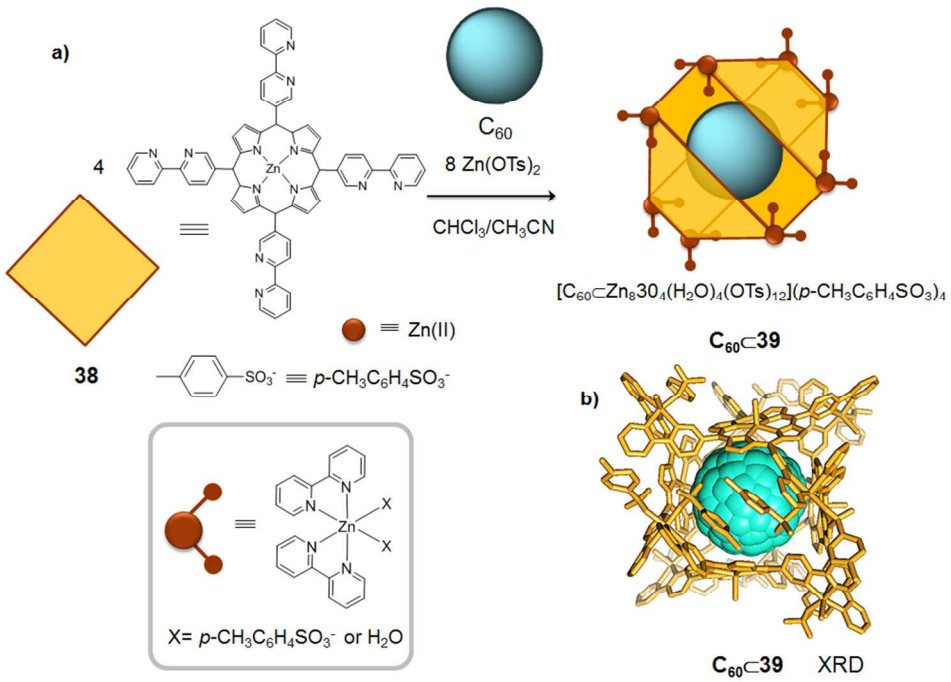

280x192mm (96 x 96 DPI)

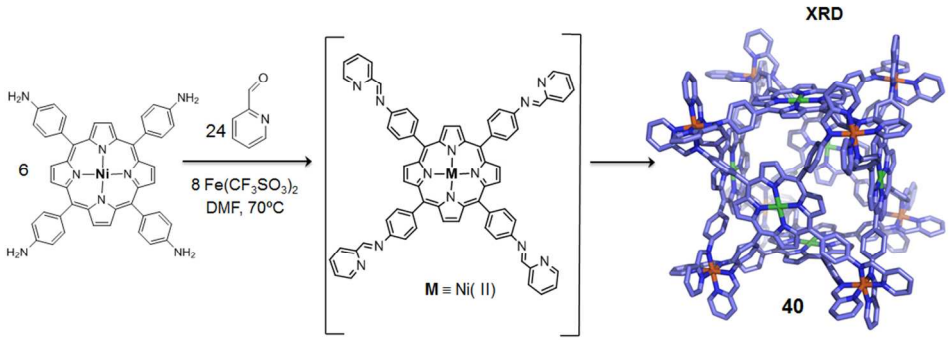

310x106mm (96 x 96 DPI)

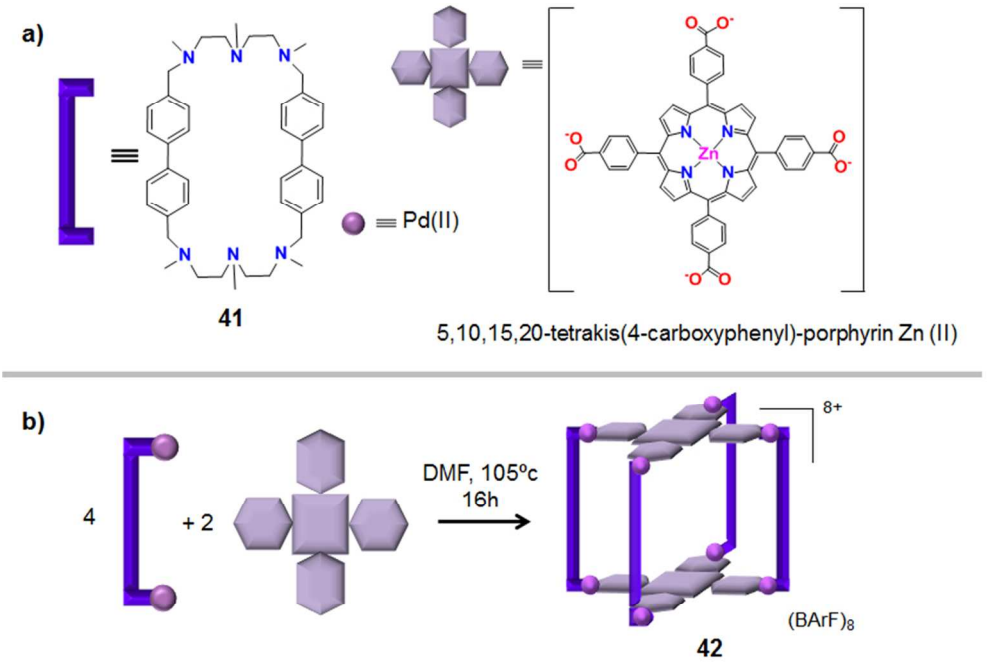

224x157mm (96 x 96 DPI)

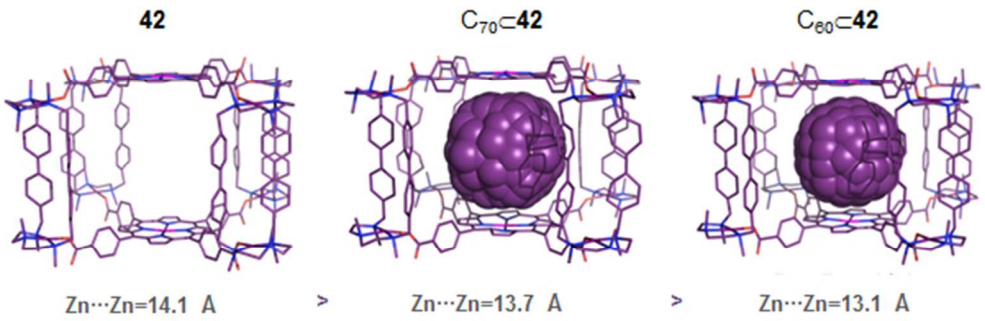

161x54mm (96 x 96 DPI)

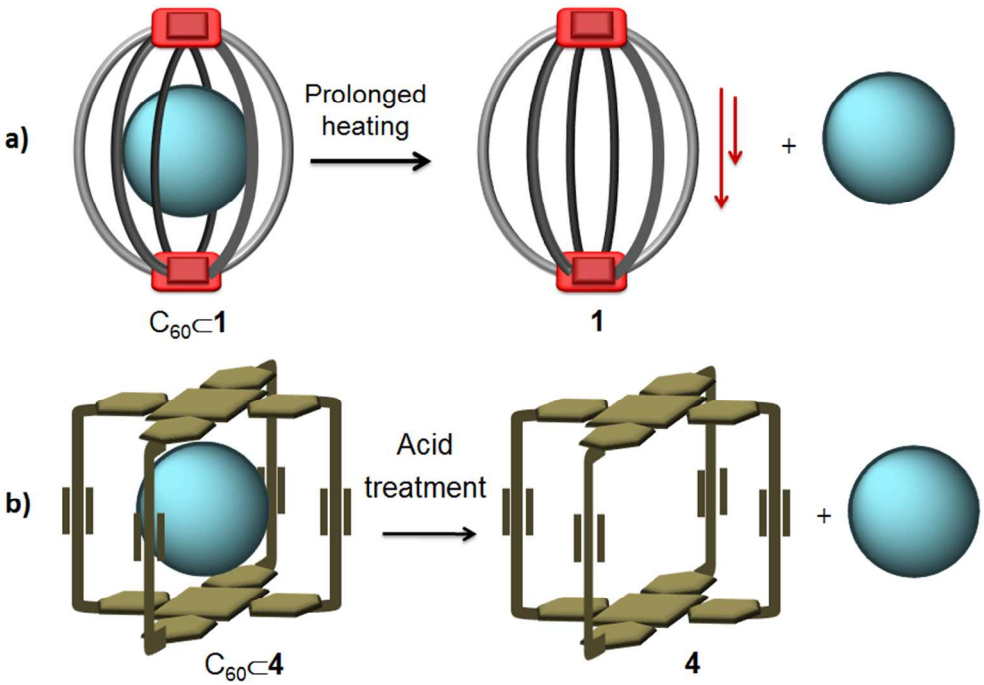

248x172mm (96 x 96 DPI)

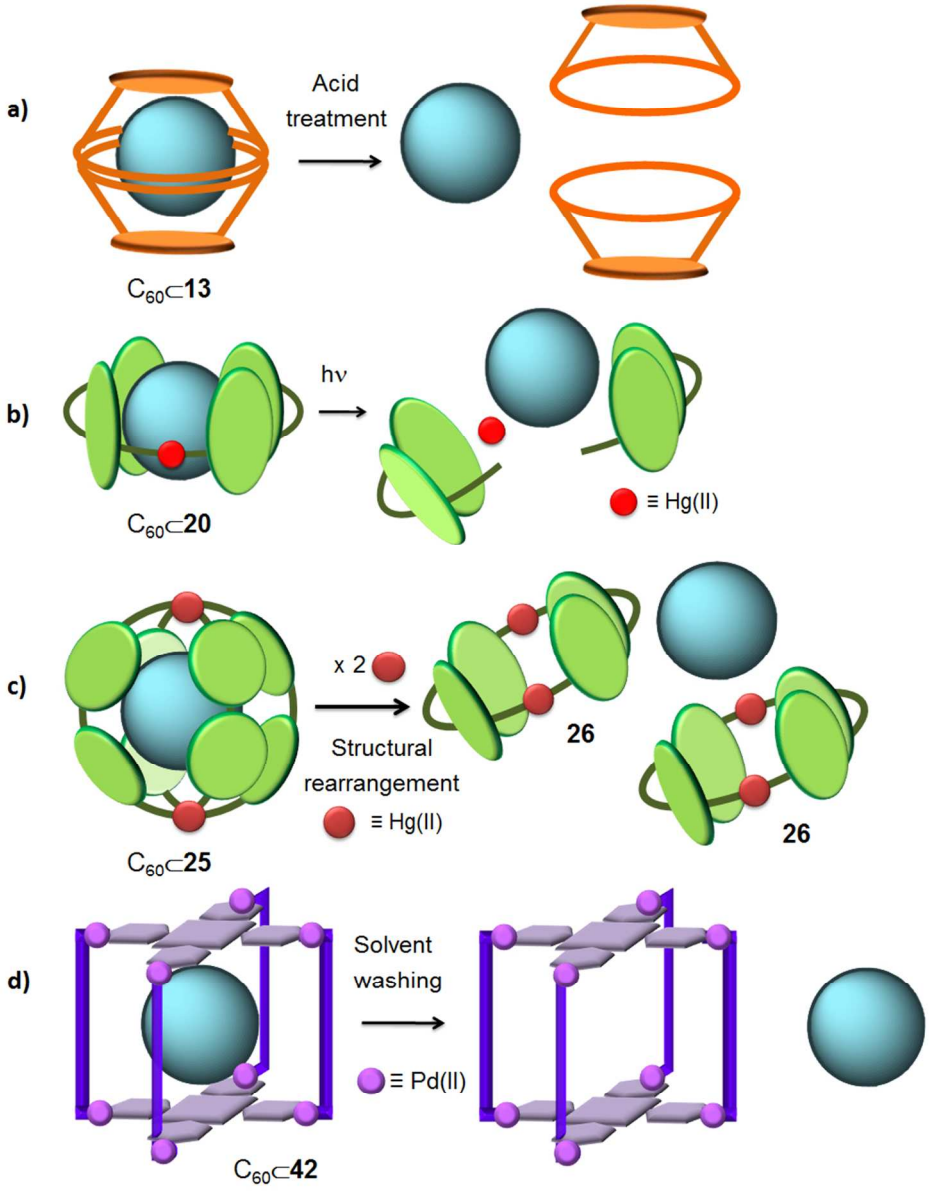

264x337mm (96 x 96 DPI)

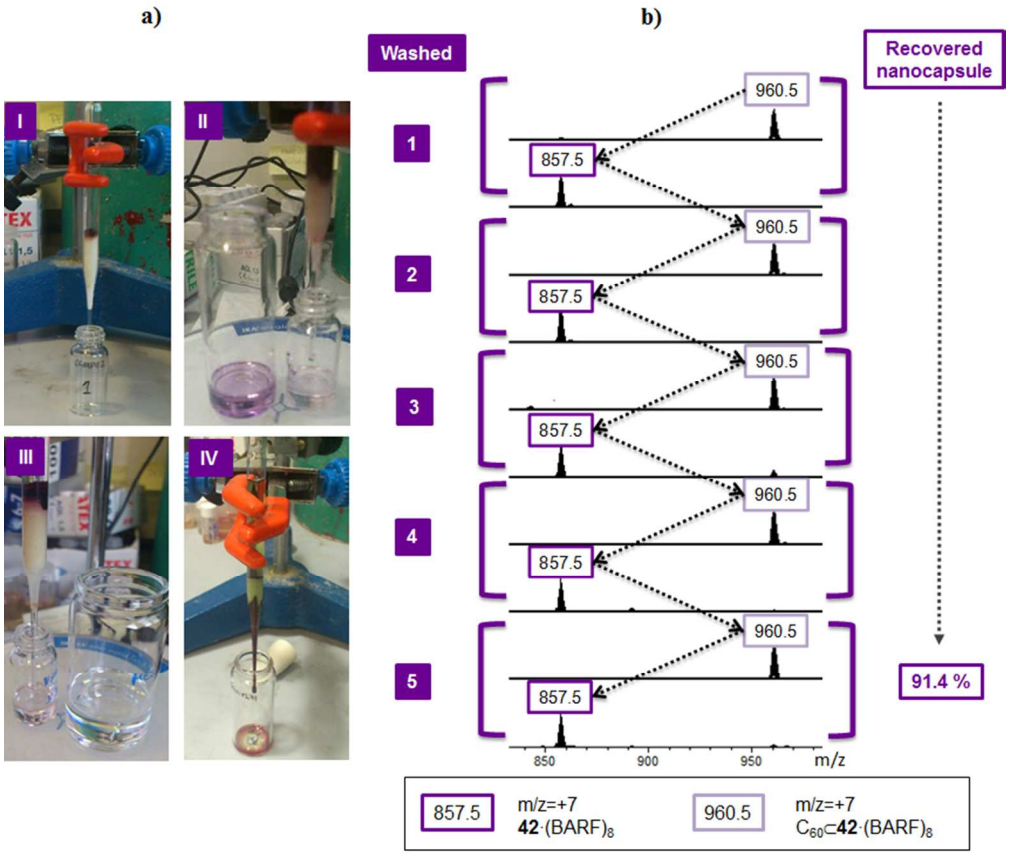

226x197mm (96 x 96 DPI)